TECHNICAL MEMORANDUM

253

Stratospheric water vapour and tropical tropopause temperatures in ECMWF analyses and multi year simulations

A.J. Simmons A. Untch, C. Jakob,
P. Kållberg and P. Undén

Research Department

April 1998

European Centre for Medium-Range Weather Forecasts
Europäisches Zentrum für mittelfristige Wettervorhersage
Centre européen pour les prévisions météorologiques à moyen

Stratospheric water vapour and tropical tropopause temperatures in ECMWF analyses and multi-year simulations

By Adrian Simmons, Agathe Untch, Christian Jakob, Per Kållberg and Per Undén[1]

European Centre for Medium-Range Weather Forecasts, Shinfield Park, Reading, UK, RG2 9AX

Abstract

The evolution of water vapour in the stratospheric analyses produced by the European Centre for Medium-Range Weather Forecasts (ECMWF) is discussed for the period since late January 1996 when the practice of resetting the upper-level specific humidity to a fixed value at each analysis time was abandoned. Very low humidities occur as expected in conjunction with deep convection and a cold tropopause over the equatorial western Pacific, where temperatures can fall below -90°C during the northern winter. There is drying in the core of the Antarctic polar night vortex where temperatures reach similarly low values. Moistening of the tropical lower stratosphere occurs predominantly in the outer tropics, where the tropopause is generally warmer. It is linked to the occurrence of strong convection and to the associated mean ascent. The tropical analyses are substantially moister in the boreal summer and autumn of 1997 than one year earlier, due in part to model changes and in part to a change in distribution of tropical convection associated with the year's strong "El Niño" event. There is a related change in the location of maximum subsequent wintertime drying.

Moisture is spread zonally and upward from the tropical tropopause, the upward transfer being insufficiently confined due to the limited stratospheric resolution of the operational 31-level model. There is significant lateral mixing within the stratosphere over the seasonal time-scale; examples are presented illustrating transfer and mixing by long- and planetary-scale waves. Significant moistening at middle and high latitudes due to mixing with more humid tropospheric air is evident only in a shallow layer at the base of the stratosphere.

Analysed temperatures near the tropical tropopause are generally in good agreement with radiosonde measurements, with standard-level biases of the order of 0.5°C or less. The past two years are the coldest by about 1°C in the tropical means of 100hPa analyses extending back to 1979. A cooling trend of about 0.6°C per decade is seen in the global mean of the 100hPa analyses. Analysed wintertime temperatures at 50hPa over the South Pole are biased warm compared with radiosonde data.

The propagation of the annual cycle in tropical stratospheric moisture is quite well represented in a multi-year simulation using a 50-level version of the model with finer stratospheric resolution and greater vertical extent. The signal moves upward at a mean rate of around 11km per year (0.35mm/s), and is attenuated realistically by mixing with the extratropics. Temperatures at the tropical tropopause and in the Antarctic polar night are accurately represented, apart from excessive persistence of cold south-polar temperatures in late winter and early spring. The latter is conducive to a drift towards an unrealistically dry model stratosphere; lack of a parametrization of upper stratospheric moistening due to methane oxidation is an obvious deficiency in this regard.

1. Introduction

There has been considerable interest and substantial progress in understanding the distribution of stratospheric water vapour in recent years. A comprehensive general review has been given by Holton *et al.* (1995), and the subject has been central to a recent Symons Memorial Lecture (Tuck *et al.*, 1997) and Presidential Address (Harries, 1997). Although confirming the classical description of the dryness and circulation of the region (Dobson *et al.*, 1946; Brewer, 1949), many subtleties have been identified concerning quantitative detail and spatial and temporal variability. Accurate simulation of water vapour in the stratosphere accordingly places a number of demands on an atmospheric general circulation model. A realistic determination of the low specific humidity of air

1. Current affiliation: Swedish Meteorological and Hydrological Institute, Norrköping.

entering the stratosphere across the tropical tropopause requires an accurate representation of several facets of deep tropical convection, of the larger-scale circulations driven by it, of the radiative processes that also play an important role in determining tropopause temperature, and of condensation at the very low temperatures typical of the region. The latter process is also active in the cold core of the Antarctic polar-night vortex. Realistic distribution of water vapour within the stratosphere requires an accurate calculation of slow mean upward transfer in the tropics, of mixing into the extratropics and of downward high-latitude transfer. This will depend on the accuracy of the model's treatment of the stratospheric wave dynamics that are involved directly in the mixing and that drive the meridional circulation responsible for the upward tropical and downward high-latitude transfer. Reasonable representations of the upper-stratospheric moistening due to methane oxidation and of mixing across the extratropical tropopause are needed to complete the picture.

When ECMWF developed its original optimum interpolation (OI) analysis system (Lorenc, 1981), it was faced with a lack of observations that could correct any drift of stratospheric humidity in the forecast model used for the data assimilation. Accordingly, it was decided simply to reset the specific humidity at each analysis time to a fixed value of 2.5mg/kg (equivalent to a mixing ratio of about 4ppmv) at all levels deemed from the temperature profile to be stratospheric. If the temperature was such that the saturation specific humidity was lower than this value, the "analysed" specific humidity was reduced to the saturated value. This was used not only in the operational production of analyses, but also in the ECMWF re-analysis of the years 1979 to 1993 (Gibson *et al.*, 1997). The resetting evidently limits the use of these analyses in the vicinity of the tropopause. For example, Ovarlez and van Velthoven(1997) noted that when the analyses are compared with aircraft measurements along flight paths that intersect the mid-latitude tropopause, they are seen to become spuriously dry on entering the stratosphere, due to their inability to represent the mixing in of moist tropospheric air that takes place in the "lowermost" stratosphere (Holton *et al.*, 1995).

The OI analysis was replaced for operational production by a three-dimensional variational analysis (3D-Var) in January 1996 (Courtier *et al.*, 1998). At the same time, the practice of resetting the stratospheric humidity at each analysis cycle was abandoned. In essence, at stratospheric levels the "background" humidity field (the six-hour forecast from the preceding analysis) is now simply used to provide the initial humidity analysis for the next forecast, unless the temperature at a point is reduced by the analysis to imply supersaturation, in which case the humidity is reduced to the saturated value at that point. The stratospheric humidity analyses thus largely evolve according to the model's dynamical and parametrized physical processes, these being constrained towards reality by the six-hourly analysis of winds and temperature. Various aspects of this evolution are discussed in this paper.

To set the scene and serve as a basis for comparison with recent months, long-term mean analysed temperatures and vertical motion near the tropical tropopause for January and July are presented and discussed in the following section. Section 3 describes a number of relevant features of the ECMWF model and analysis system, and sections 4 and 5 discuss respectively some analysis and modelling problems which have been encountered and remedied since January 1996. The next section discusses variations in the analyses of specific humidity near the tropical tropopause since April 1996, after the worst of the aforementioned problems had been corrected. It is followed in section 7 with an account of how changes in humidity introduced at the tropical tropopause are spread throughout that portion of the stratosphere resolved by the assimilation system. Discussion of exchange across the extratropical tropopause is included in this section. The accuracy and variability of analysed temperatures at the tropical tropopause and at 50hPa at the South Pole in winter are discussed in section 8. An account of the evolution of stratospheric water vapour in multi-year simulations is given in the next section, which shows in particular how increasing the vertical resolution and extent of the model stratosphere brings a substantial improvement to the representation of the upward migration and attenuation of the annual cycle in tropical stratospheric humidity, the "tape recorder effect" discussed by Mote *et al.*(1996). A concluding discussion is presented in section 10.

2. MEAN ANALYSED TEMPERATURES AND VERTICAL MOTION NEAR THE TROPICAL TROPOPAUSE

Fig. 1 presents temperature and vertical motion averaged for January and July over the period 1979-1993, based on the ECMWF re-analyses. The January maps are shown for the model level that lies close to 90hPa, where the coldest mean analysed tropical temperatures are generally found during the boreal winter. The July maps are shown both for the 90hPa level and for the model level below, which is close to 110hPa. The location of the 31 model levels used for the re-analysis and in operations since September 1991 is shown in Fig. 2, and discussed further in the following section. The fields shown in Fig. 1 have been averaged over all six-hourly analyses to remove diurnal and semi-diurnal tidal features. In addition, the vertical motion fields have been smoothed by truncating their archived T106 spherical-harmonic representations to T15, to remove stationary small-scale orographic features and any local effects of inconsistent data from individual observing stations.

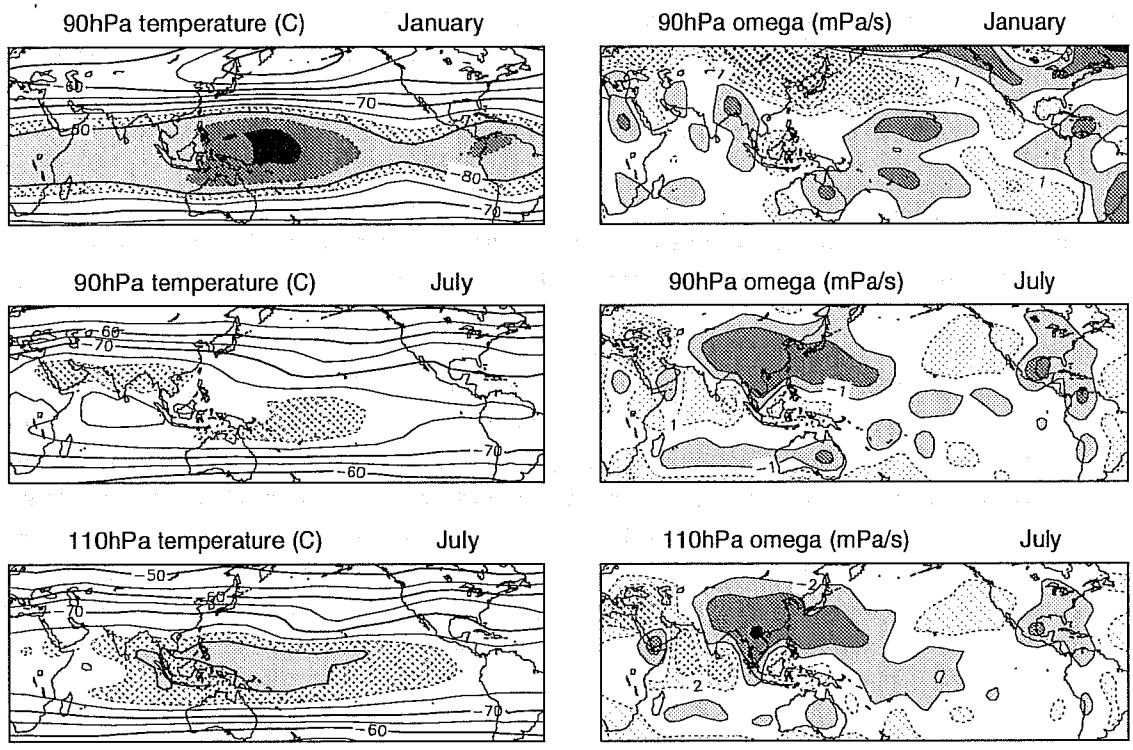

Figure 1 Temperature (left) and vertical motion (right) averaged for January at 90hPa (upper) and for July at 90hPa (middle) and 110hPa (lower) for the period 1979-1993, based on ECMWF reanalyses. Temperature is plotted with a contour interval of 5°C in the unshaded regions (for temperatures above -77.5°C) and 2.5°C in the shaded regions. The darkest shading denotes temperatures below -85°C. The contour intervals for vertical motion are 1, 3 and 9mPa s^{-1} for the 90hPa level and 2, 6 and 18mPa s^{-1} for the 110hPa level, with solid contours and solid shading denoting ascent, and dotted contours and stippled shading denoting descent.

The coldest tropopause temperatures in January normally occur over the tropical western Pacific, migrating towards the central Pacific at times of El Niño, as will be illustrated later. The minimum temperature is lower than -85°C in the fifteen-year mean. The coldest region is also one of mean ascent, both features being linked with the strong deep convection that occurs in conjunction with particularly warm sea-surface temperatures. This is the region of the "stratospheric fountain" (Newell and Gould-Stewart, 1981) where the driest air enters the stratosphere. Extensive evidence reviewed by Holton *et al.*(1995) points to the actual drying as being associated more with processes near the tops of the deepest, overshooting, convective systems than with the large-scale ascent. The January map also shows a region of relatively cold temperatures and ascent over central America.

Temperatures are less cold in July than January over almost all the tropics. The lowest values are again found over the tropical western Pacific, with a minimum below -80°C at the110hPa level. This is also a region of mean ascent, although there is much stronger ascent over south-east Asia and eastward into the subtropical western Pacific, associated with the Asian summer monsoon. Descent occurs over the Middle East and eastern Mediterranean (as discussed by Rodwell and Hoskins, 1996) and over the northern Indian Ocean. July temperatures are analysed to be slightly colder at 90hPa than at 110hPa over the southern Asian land mass. Another feature of the July means is a region of ascent over central America, which occurs where the tropical tropopause is warmest.

Much more confidence can be placed in the directly analysed temperature fields (whose accuracy is discussed later) than in the derived vertical motion fields, especially near the tropopause. Idealized calculations of the stationary tropical motion forced by an imposed steady tropospheric heating show virtually no response at stratospheric levels (Simmons, 1982), and Holton *et al.*(1995) argue that a circulation forced from below with a temporal variation on the annual time-scale will penetrate only a few kilometres into the stratosphere. The mean analysed vertical motion for July is plotted with contour intervals twice as large at 110hPa than at 90hPa in Fig. 1, and can be seen generally to more than halve in magnitude between 110 and 90hPa. The mean ascent in January over the tropical western Pacific decreases even more rapidly with increasing height. This sharp decrease in the intensity of the convectively-driven large-scale ascent (and descent) near the tropopause raises a question as to whether the 20hPa vertical resolution of the assimilating model around the 90hPa level is sufficient to give a reliable indication of the strength of the mean vertical motion near this level. Indeed, part of the motivation for examining the realism of the distribution of stratospheric water vapour in the analyses is the indication provided of the accuracy of other components of the model and analyses, the vertical motion being an example.

The results discussed later in this paper indicate that convection indeed plays an important role in determining the distribution of humidity near the tropical tropopause, but there are also indications of a part played by the associated mean ascent and descent. Although there is uncertainty as to the extent that such mean vertical motion influences local transfer at the base of the tropical stratosphere, there is nothing in the results presented here to question the view that the mean upward transfer of water vapour further above the tropical tropopause is due to the large-scale ascent forced in the tropical stratosphere by the "wave-driven extratropical pump" mechanism reviewed by Holton *et al.*(1995). Moreover, linking the region of cold tropopause temperatures with that of strong tropical convection and warm sea-surface temperatures is not inconsistent with the arguments of Yulaeva *et al.* (1994) that the annual variation in the *zonal-mean* height and temperature of the tropical tropopause is largely controlled by the stratospherically forced mean circulation.

3. THE ECMWF FORECASTING SYSTEM

The basic numerical formulation of the global ECMWF model used in operations since September 1991 has been described by Ritchie *et al.*(1995). The primary dynamical variables are represented spectrally, with the spherical harmonic expansions truncated triangularly at total wavenumber 213 (T213). The associated computational grid has a quasi-regular spacing of about 60km in longitude as well as latitude. It was originally the "fully reduced" Gaussian grid defined by Hortal and Simmons(1991), but was modified slightly in April 1995 following Courtier and Naughton(1994). The code of the model was changed completely in 1994 to use software developed jointly with Météo-France (Courtier *et al.*, 1991). The original three-time-level semi-Lagrangian advection scheme described by Ritchie *et al.* was used operationally until December 1996, when it was replaced by a two-time-level scheme (Simmons and Temperton, 1997). The multi-year simulations reported later were carried out using the three-time-level scheme and T63 resolution.

The model uses a hybrid vertical resolution which reduces smoothly from a terrain-following coordinate at low levels to a pressure coordinate in the lower stratosphere (Simmons and Burridge, 1981; Simmons and Strüfing, 1983). The 31-level resolution used operationally is illustrated in the left-hand portion of Fig. 2; the right-hand portion shows the 50-level resolution used for the main multi-year simulation. The uppermost four levels of the 31-level version are located precisely at pressures of 10, 30, 50 and 70hPa, and the pressures at the next two levels depend only slightly on surface pressure, being within 0.1hPa of 90hPa and 1hPa of 110hPa. These two levels will be referred to as simply the 90hPa and 110hPa levels. The resolution of the 50-level version is identical to that of the 31-level version below 150hPa. Levels are approximately equally-distributed in height with a spacing of about 1.5km between about 60 and 5hPa. The spacing increases above the 5hPa level and the top level is at 0.1hPa. This configuration of levels was determined experimentally as the minimum enabling a reasonable-looking simulation of the quasi-biennial oscillation (QBO) in the tropical stratosphere (Untch, 1998). The 50-level version of the model includes a Rayleigh friction at the uppermost four levels with a damping rate which is prescribed analytically to increase from zero at 1hPa, and which has a value of $(3.3\text{days})^{-1}$ at 0.1hPa.

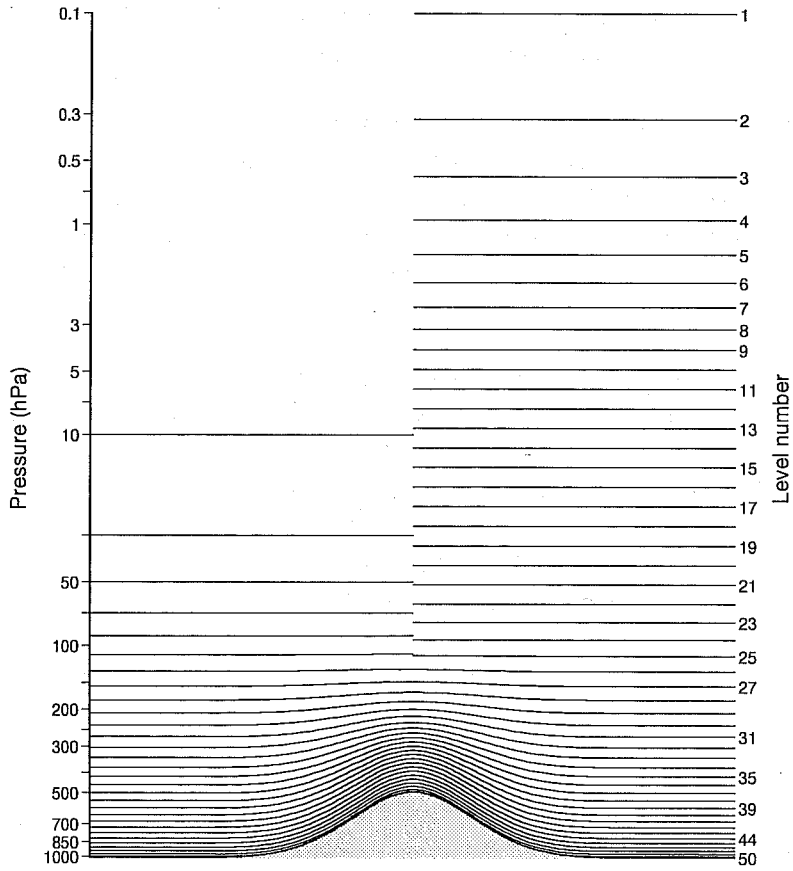

Figure 2 The distribution of full model levels for 31-level (left) and 50-level (right) vertical resolutions, plotted for a distribution of surface pressure which varies from 1013.25 to 500 hPa.

Since April 1995, the specific humidity in the model has been represented not spectrally, but by its values at the computational grid points, following Williamson(1990). A "quasi-monotone" version of the semi-Lagrangian advection is used. The general semi-Lagrangian algorithm requires computation of interpolated values for specific humidity (and other advected variables) at the departure points of trajectories that finish one time-step later at the grid points. In the quasi-monotone approach (a revision of that proposed by Bermejo and Staniforth, 1992), each of a sequence of one-dimensional cubic interpolations is limited so that the interpolated value is within the range defined by the field values at the two surrounding grid-points (Hortal, 1994). No explicit horizontal diffusion is

applied to the specific humidity. The change to this new treatment of specific humidity was accompanied by introduction of the quasi-monotone scheme for the horizontal interpolations of temperature and winds. The scheme was not applied to the vertical interpolations of these variables because this was found to cause undesirable reductions in sharp minima and maxima, notably at the tropical tropopause in the temperature field and at the wind maximum associated with the QBO.

The model's mass-flux parametrization of convection (Tiedtke, 1989) is linked to a prognostic cloud scheme (Tiedtke, 1993), providing a representation of the processes believed to be important for transfer across the tropical tropopause. Deep convection can overshoot the level of zero buoyancy and detrain cloud ice into stratiform (anvil) clouds which may either precipitate or evaporate depending on ambient conditions. Precipitation may evaporate at lower, subsaturated levels. Since December 1996, the model clouds have been advected using the same numerical scheme as applied to specific humidity. Though developed for tropospheric conditions, the cloud scheme is applied throughout the model, and thus becomes active when temperatures in the wintertime Antarctic stratosphere become cold enough to trigger the condensation process. Although there is little doubt from observations that the parametrized cloud processes do occur in the Antarctic winter vortex (Tuck *et al.*, 1997), the accuracy of the scheme as applied to stratospheric conditions must be open to question.

The other parametrization schemes active in the model stratosphere are the radiation (Morcrette, 1990) and gravity-wave drag (Lott and Miller, 1997). The latter deals only with the drag associated with waves forced by subgrid-scale orography. There is no parametrization of drag due to gravity waves excited by other sources. More importantly in the present context, there is also no parametrization of moistening of the stratosphere by methane oxidation. The set of major parametrizations is completed by a boundary-layer scheme (Beljaars, 1995) and a land-surface scheme (Viterbo and Beljaars, 1995).

In November 1997, a four dimensional variational version of the data assimilation scheme (4D-Var; Rabier *et al.*, 1998b) replaced the 3D-Var scheme introduced in January 1996. The 3D-Var scheme had previously been extended in September 1996 in the areas of observation screening (Järvinen and Undén, 1997), quality control (Andersson and Järvinen, 1998) and background-error variance calculation (Fisher and Courtier, 1995). A new formulation of the background error constraint was introduced in May 1997 (Bouttier *et al.*, 1997). With 3D-Var, analyses were produced for the main synoptic hours of 00, 06, 12 and 18UTC, based on six-hour background forecasts from the preceding analysis. Observations in a six-hour window centred on the analysis time were used as if valid at the analysis time. The first operational version of 4D-Var uses the same six-hour observation window, but uses the observations in one-hour slots, producing initial conditions for the model at 03, 09, 15 and 21UTC which provide the best fit of the ensuing six-hour forecast (the "final trajectory") to the observations. For continuity, and as many types of observation are concentrated at the main synoptic hours, the final-trajectory forecasts at three-hour range are regarded as analyses for the main synoptic hours. At six-hour range they provide the background fields for the next analysis.

In the variational analysis, whether 3D- or 4D-Var, a cost function (a sum of terms representing deviations from the background state, deviations from the observations and a weak gravity-wave constraint) is minimized jointly for temperature, winds and specific humidity. The minimisation procedure determines lower resolution (T63) spectral representations of the deviations of all analysed fields (including humidity) from their background values. These "analysis increments" are added to the high resolution background fields to form the analysis.

Background errors in humidity are assumed to be uncorrelated with background errors in temperature or wind, although the specified variance of humidity errors depends on the background temperature. Direct radiosonde measurements of humidity (which are generally considered unreliable in very dry conditions) are used only at or

below 300hPa. TOVS[1] radiance data are also used; they are matched in the analysis by simulated radiances which depend on model humidity values only from levels below 300hPa (McNally and Vesperini, 1996). Analysis increments are nevertheless produced at higher levels through the specified vertical correlation of background humidity errors (Rabier *et al.*, 1998a). Moreover, the minimization may adjust the humidity field as well as the temperature field at any model level when matching the standard-level geopotential heights from radiosondes. The minimisation is performed without constraints that the humidity field be positive and not supersaturated; these are simply imposed in the final step of the analysis, after increments have been added to the background fields.

Some specific problems encountered with the above procedure are documented in the following section. This is followed by discussion of the recent model changes that most affected the stratospheric humidity. In general, changes to the operational forecasting system at ECMWF (as elsewhere) are finally tested by starting the test system from an operational analysis and running on in parallel with subsequent operations for a number of weeks or months. The parallel test stream is then switched in real time to become the new operational stream. To avoid the jumps that this causes in long sequences of operational analyses of sensitive fields such as tropopause humidity, results in this paper are presented from parallel test analyses rather than operational analyses for periods of overlap. In particular, all results for dates from 1 September 1997 onwards are from 4D-Var analyses.

4. EARLY ANALYSIS PROBLEMS

Soon after 3D-Var became operational, it was realised that the global-mean stratospheric humidity was drifting slowly towards unrealistically moist values. This was traced to the fact that the covariances between humidity at levels where observations were used and humidity at levels near the top of the model, though very small, were not exactly zero. A combination of an overall moist bias of background humidity compared with observations and a negative correlation between tropospheric humidity errors and humidity errors above 100hPa led to the moistening. This problem was addressed by a change made in March 1996 in which correlations between levels below and above 100hPa were set to zero. As a precaution against a stratospheric humidity change when fitting the radiosonde height data, the background humidity error was set to a very small value above 150hPa. When the change was made, specific humidities larger than 2.5mg/kg were reduced to this value in a one-off procedure. This caused little change near the tropical tropopause, where the model's representation of the natural drying process had been strong enough to prevent serious drift due to poor analysis technique. The evolution of the humidity field near the tropical tropopause and in the stratosphere above 100hPa will be discussed further only from 1 April 1996 onwards.

Although the above change cured the most widespread problem, it did not remove a drying in the lower polar stratosphere below 150hPa. In this case the drying increments produced by observations in the upper troposphere were spread upward into the lowermost polar stratosphere by positive error-correlations. In December 1996, the analysis was changed to suppress addition of humidity increments where the background specific humidity was lower than 5mg/kg. This effectively prevents any effect of the analysis from being felt at dry stratospheric levels, apart from removal of any supersaturation that occurs if the analysis lowers the temperature where the background is close to saturated. This may happen typically near the tropical tropopause or in the Antarctic stratospheric winter vortex.

Because of these problems, extreme caution must be exercised when using operational upper-level humidity analyses retrieved from the ECMWF archives for most dates in 1996.

1. TIROS (Television Infra-Red Observation Satellite) Operational Vertical Sounder

5. SENSITIVITY TO MODEL CHANGES

Two of the changes made to the operational ECMWF model since January 1996 have had a significant effect on the stratospheric humidity. The first entailed correction of a coding error in the treatment of detrainment by the convection scheme. Routine tests of the change had classified it as a minor one, but it was subsequently found to have caused a substantial moistening of analyses near the tropical tropopause, and it can be assumed to have led eventually to a substantial moistening of the stratospheric analyses as a whole. The second change was prompted directly by investigations into the realism of very low values of specific humidity found near the tropical tropopause in the analyses for 1996. It involved improvement to the calculation of the saturation specific humidity at low temperatures, which also resulted in a moistening.

The first change was made together with a revision to the treatment of the stable boundary layer and introduction of freezing of soil-water, these other changes being highly unlikely to have contributed materially to the moistening of the tropical tropopause. This set of parametrization changes was added to an existing parallel suite, which was being used to test analysis changes (referenced earlier) necessary for an operational changeover of computer systems in September 1996. Fig. 3 shows that the tropical-mean specific humidity at 90hPa was some 25% higher after about 20 days of assimilation with the new version of the parametrizations. This is clear evidence of the importance of the convective detrainment mechanism in determining the degree of dryness of the analyses near the tropical tropopause. Over the test period, both sets of 90hPa analyses were dried in the deep tropics, predominantly over the western Pacific where the tropopause was coldest. They were moistened in the outer tropics and subtropics, notably over the western Pacific and over the western Atlantic and Caribbean, in part associated with the tropical cyclones that are typically present in these regions at this time of year. Examples of similar drying and moistening will be illustrated later for other months. The change to the convection scheme produced both less drying in the deep tropics and more moistening further from the equator.

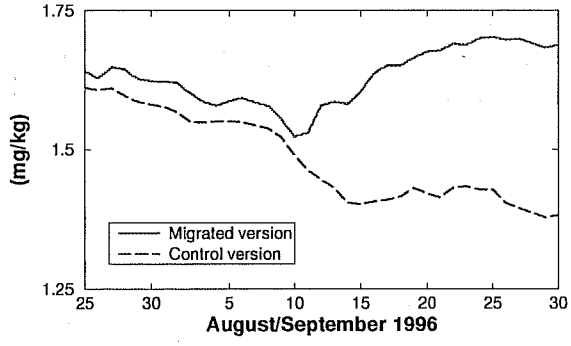

Figure 3 Variation from 25 August to 30 September 1996 of tropical-mean specific humidity analyses (mg/kg) at the 90hPa model level. The dashed curve shows the result from the "Control" version of the data assimilation system run on the computer system used for operational production until 16 September 1996, and the solid curve shows that from the "Migrated" version run on the computer system that took over operational production on 18 September 1996. The parametrization of convective detrainment was corrected in the migrated version on 10 September 1996.

The physical parametrization schemes in the operational ECMWF model use a Tetens (or Magnus) formula to compute the saturation vapour pressure, $e_s(T)$, as a function of temperature, T. The saturation specific humidity, $q_s(T,p)$, is given in terms of $e_s(T)$ by:

$$q_s(T,p) = \frac{\varepsilon e_s(T)}{p-(1-\varepsilon)e_s(T)}$$

where ε is the ratio of the specific heats of dry air and water vapour, approximately 0.622. The formula for $e_s(T)$ is:

$$e_s(T) = a_1 e^{a_3\left(\frac{T-T_0}{T-a_4}\right)}$$

where T_0=273.16K and T is in degrees Kelvin. The parameters a_1, a_3 and a_4 were changed in August 1997 to increase the accuracy of $e_s(T)$ at low temperatures. At the same time, the calculation of $e_s(T)$ used by the analysis scheme was changed to be the same as that used by the model. Details are given in an Appendix to this paper.

This second model change increased the specific humidity of air entering the stratosphere through the tropical tropopause by some 10 to 15%, and caused a similar moistening of air in the cold core of the polar-night vortex in the Antarctic wintertime stratosphere. This moistening was clearly identified in initial test forecasts and analyses in which the only change was in the calculation of the saturation vapour pressure. Results are presented in Fig. 4 from a final pre-operational test period in which the revised calculation was included with a number of other model and analysis changes. The impact of the new version of the forecasting system is shown in time series of the specific humidity averaged over the tropics at 90hPa and over the polar cap south of 70°S at 50hPa. Both regions are moistened as expected. It should, however, be noted that differences shown in Fig. 4 are likely also have been influenced by some of the other changes introduced at the time. These changes included use of a new ozone climatology and direct use of TOVS radiances above as well as below 100hPa. Previously retrievals rather than radiances were used above 100hPa in the extratropics, and no satellite data was used in the tropical stratosphere. The new analyses were on average warmer by 0.7°C at 50hPa over the polar cap and cooler by 0.2°C at 90hPa in the tropics.

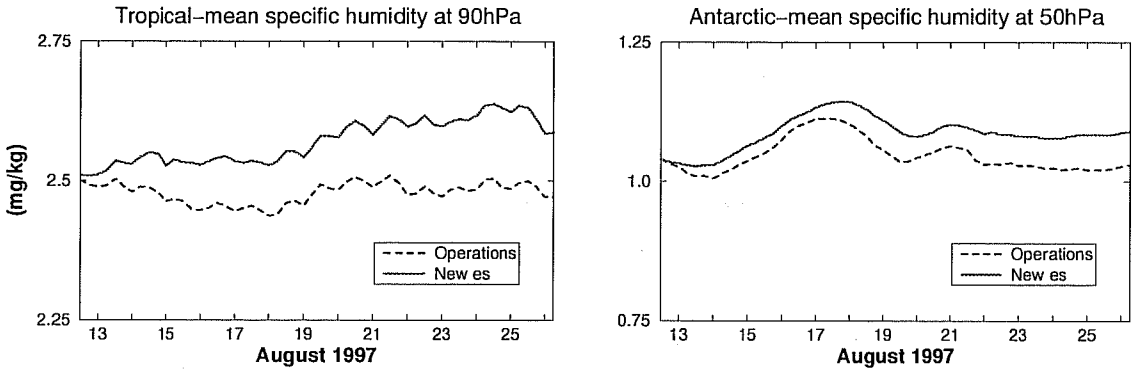

Figure 4 Variation with time of the tropical-mean specific humidity at the 90hPa model level (left) and of the specific humidity at the 50hPa level averaged over the polar cap south of 70°S (right). The dashed curves denote the operational analyses for the period from 13 to 26 August 1997, and the solid curves denote analyses from a trial version of the data assimilation system that became operational on 27 August 1997. The trial version included the revised calculation of saturation vapour pressure.

A further substantial model change was made in December 1997. This involved revisions to ice-cloud optical properties and several other aspects of the radiation scheme, a new closure of the convection scheme and a modified fallout of ice in the cloud scheme. Changes in these areas could have had a significant impact on the entry of water vapour into the model stratosphere, but were found to cause a net drying at the tropical tropopause of only around 3% over a three-week period of pre-operational parallel running. The tropics were cooled in the mean at 90hPa by the change, but by less than 0.2°C.

6. WATER VAPOUR NEAR THE TROPICAL TROPOPAUSE

Fig. 5 shows the tropical-mean specific humidity from 90hPa analyses for the period from April 1996 to February 1998. The analyses evidently reproduce the annual cycle in water vapour clearly seen in measurements from the

Upper Atmosphere Research Satellite (UARS; Mote *et al.*, 1996; Harries, 1997). The analyses in the boreal summer and early autumn of 1996 are substantially drier than one year later, even when values are scaled to account for the model changes discussed in the preceding section. 1996 also stands out as the driest year of the period 1992-1996 in retrievals of water vapour at 100hPa from the Halogen Occultation Experiment (HALOE) on UARS (Harries, *loc. cit.*). A number of adjustments are needed to make quantitative comparison with the 100hPa climatology from HALOE derived by Jackson *et al.*(1998). Apart from allowance for the model changes, analysed values need to be increased by some 15% to account crudely for the difference between values at 90 and 100hPa (see below) and multiplied by 1.6 to convert specific humidity (in mg/kg) to volume mixing ratio (in ppmv). Thus scaled, the analyses indicate a tropical-mean100hPa mixing ratio of about 3ppmv in boreal winter and 4-5ppmv in late summer. These values are in reasonable agreement with the HALOE climatology, especially given the uncertainties in the scaling, in the effect of interannual variability and in the accuracy of the retrievals. It would be surprising if the humidity analyses do not contain some significant remaining flaws near the tropical tropopause, but they appear realistic enough in overall magnitude to justify more detailed examination, particularly as they provide a coverage and resolution in space and time that is unavailable from either satellite or *in situ* measurements.

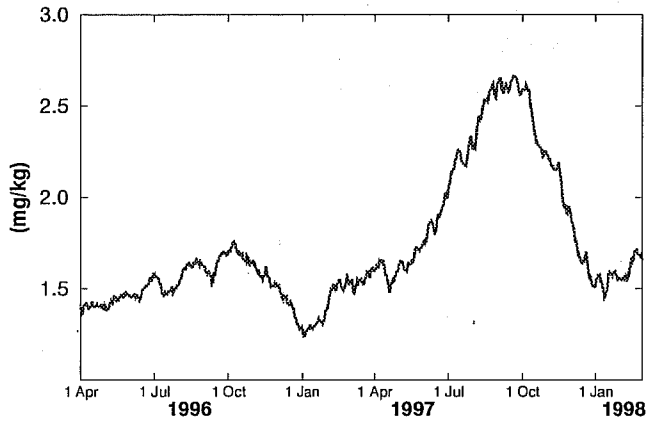

Figure 5 Variation of the tropical-mean specific humidity at the 90hPa model level from 12UTC ECMWF analyses for the period from 1 April 1996 to 28 February 1998.

Some monthly-mean fields for July 1996 and July 1997 are presented in Fig. 6. Results are shown at both 90hPa and 110hPa. Comparison with Fig. 1 indicates that the July tropopause is higher and colder in the analyses for 1996 and 1997 than in the mean for 1979-1993, a result to which we shall return in section 8. Specific humidities are typically some 30% higher at 110hPa than at 90hPa in the tropics (leading to the 15% scaling factor in converting from 90 to 100hPa values above).

Some pronounced differences between July 1996 and July 1997 can be seen in Fig. 6, quite apart from an overall moistening ascribable to the model change in September 1996. Several of these differences appear to be consequences of a different distribution of convection associated with the El Niño event that was in progress during July 1997. The region of minimum tropopause temperature is located further east over the Pacific in 1997 and is warmer than one year earlier. Mean descent is more evident over Indo- and Micro-nesia. A band of mean ascent stretches across the northern tropical Pacific Ocean and into the Caribbean in 1997, apparently associated with stronger and more broadly distributed rainfall along the inter-tropical convergence zone. A maximum in specific humidity occurs over southern Asia in both years; in 1997 there is also a maximum over the Caribbean, where tropopause temperatures are relatively warm. There is no evidence in the analyses for July 1997 of the dry band that extends from the equatorial western Pacific over the Indian Ocean and into Africa in the corresponding analyses for 1996. Daily maps indicate that this band arises from repeated instances of convective drying, predominantly in the region of coldest mean tropopause temperature. The driest air is located further west at

110hPa than at 90hPa, and further west still at the next lower model level (close to 130hPa, not shown). Corresponding maps have been examined for August, September and October 1996, and they present a similar picture over the Indian Ocean.

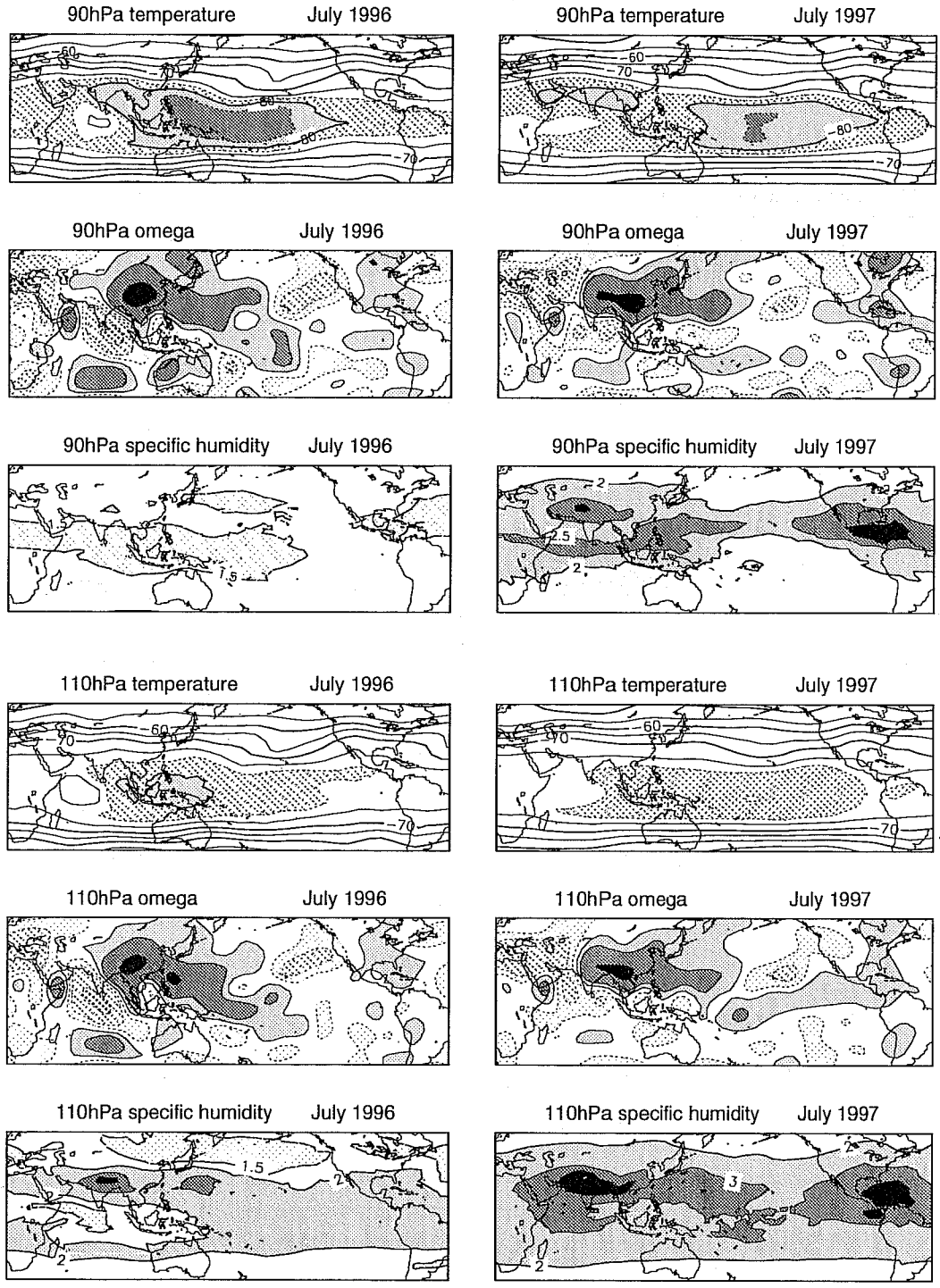

Figure 6 Temperature, vertical motion and specific humidity at 90hPa (upper panels) and 110hPa (lower panels) averaged over analyses for July 1996 (left) and July 1997 (right). Contouring and shading for temperature and vertical motion are as in Fig. 1. For specific humidity, solid contours and solid shading denote relatively moist areas, with contour values 2, 2.5 and 3mg/kg for the 90hPa level and 2, 3 and 4mg/kg for 110hPa. The darkest shading denotes the highest humidity. Stippled areas enclosed by dotted contours denote relatively dry values in the range 1-1.5mg/kg.

The high analysed values of near-tropopause specific humidity well north of the equator in boreal summer, with a maximum over southern Asia, are in good agreement with the retrievals of HALOE data presented by Harries(1997) and Jackson *et al.*(1998). A secondary maximum in water vapour near central America in summer and autumn is also seen in the results from HALOE. In addition, the observations indicate a dry region over the Indian Ocean in these seasons. This is located further to the west in retrievals at 128hPa than in those at 100hPa, and the driest region is over Indonesia in retrievals at 83hPa. Our results for 1996 suggest that this pattern is due to strong convective drying at the cold, high tropopause over Indonesia, with westward, descending flow carrying the dry air out and down over the Indian Ocean.

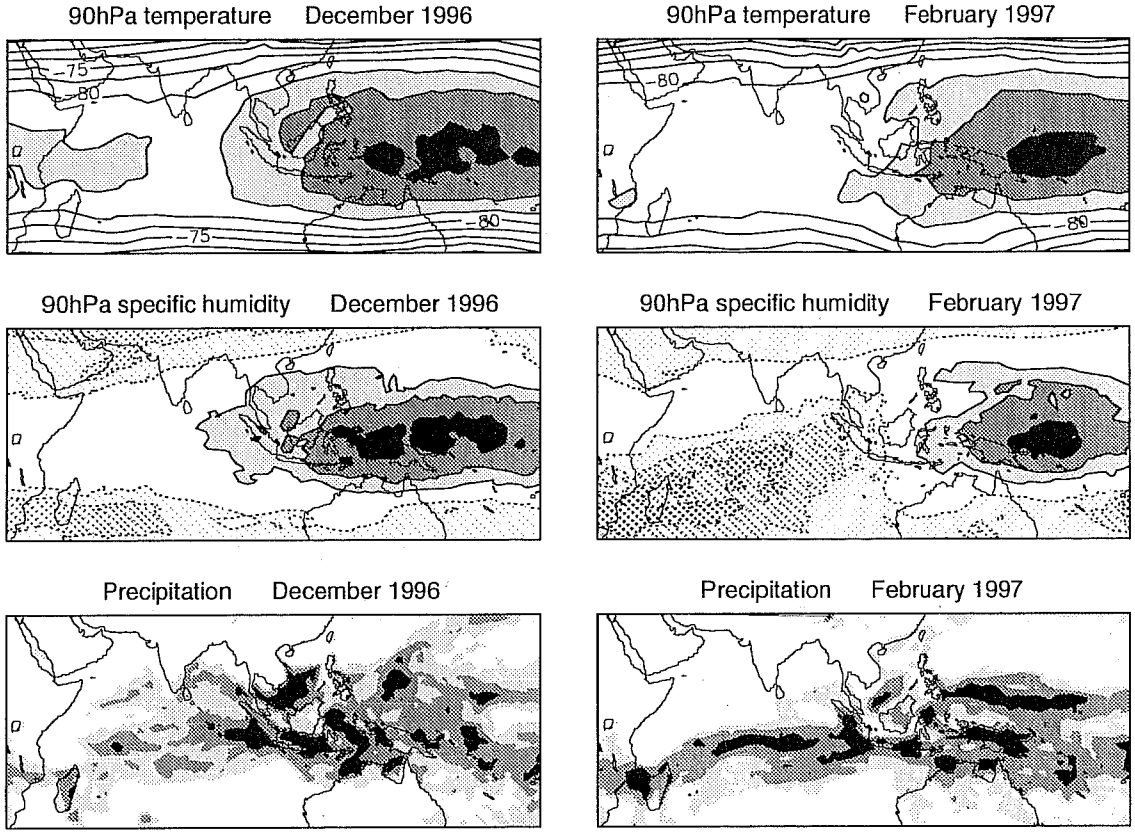

Figure 7 Temperature (upper) and specific humidity (middle) at 90 hPa and precipitation (lower) averaged for December 1996 (left) and February 1997 (right). Temperature and specific humidity are averages of 12UTC analyses; precipitation is average of 24-hour forecasts starting from 12UTC analyses one day earlier. The contour interval for temperature is 2.5°C, with shading for temperatures below -82.5°C. For specific humidity, solid contours and solid shading denote relatively dry areas, with contour values 1.2, 1 and 0.8mg/kg. The darkest shading denotes the lowest humidity. Stippled areas enclosed by dotted contours denote relatively moist areas, with contour values 1.6, 1.75 and 1.9mg/kg. Shading limits for precipitation are 4, 8 and 16mm/day, with darkest shading indicating heaviest precipitation.

Fig. 7 presents some monthly-mean fields for December 1996 and February 1997. There is a clear similarity between the two monthly means over Micronesia, where at 90hPa there are both very cold temperatures (with minima below -88°C) and very low specific humidities (with minima below 0.8mg/kg). There is, however, a marked difference between the two months in specific humidity over the Indian Ocean. Analyses near the tropopause are considerably moister over this region in February. Mean distributions of precipitation (from 24-hour forecasts, included in Fig. 7) also show a marked difference between the two months over the Indian Ocean. The convection in February is strong and much more localized in a band extending from Indonesia to Madagascar and southern Africa. The band marks the track of the tropical cyclones active in this month. This convection is effective in the model in moistening the analyses near the tropopause, in a way similar to that noted earlier for the northern

tropics and subtropics over the western Pacific and Atlantic in September 1996. East of Australia, the map of specific humidity for February shows the edge of a further region of convective moistening, which extends eastward close to the Tropic of Capricorn.

A further feature of the analyses for February 1997 is that there tends to be more moistening at 70hPa (not shown) than at 90hPa over the eastern Indian Ocean and Indonesia. If convection overshoots the model tropopause at 90hPa there will be some detrainment at the next higher level, 70hPa. There can be more moistening here than at 90hPa if ambient conditions are close to saturation at 90hPa and significantly subsaturated at 70hPa (where the saturation specific humidity will generally be higher because of both higher temperatures and lower pressure). Observational evidence for moistening above the tropopause by evaporation of ice particles at the top of deep convection has been presented by Vömel *et al.*(1995). The present results must nevertheless be treated with some caution, as the model's coarse vertical resolution of close to 20hPa near the tropical tropopause may result in a direct convective moistening at too high a level in the lower stratosphere.

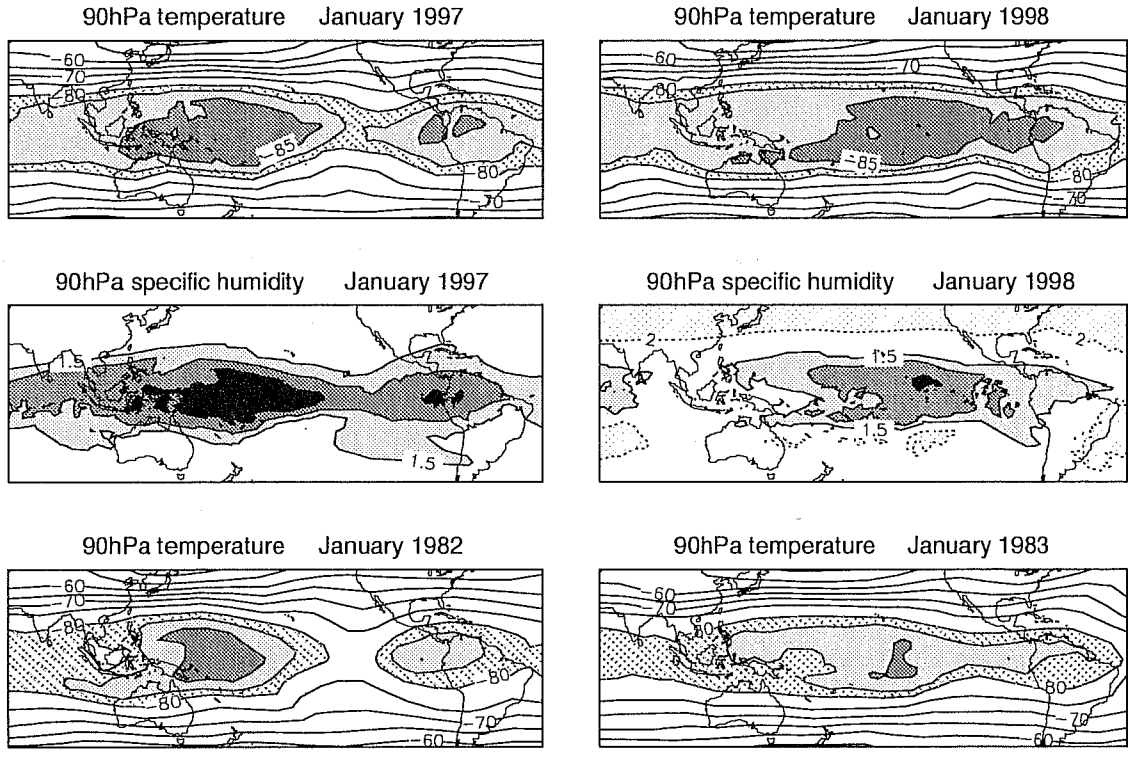

Figure 8 Mean temperature (upper) and specific humidity (middle) analyses at 90 hPa for January 1997 (left) and January 1998(right), and mean temperature (lower) at 90hPa for January 1982 (left) and January 1983 (right). The contour interval for temperature is 5°C in the unshaded regions (for temperatures above -80°C), and 2.5°C in the shaded region. For specific humidity, solid contours and solid shading denote relatively dry areas, with contour values 1.5, 1 and 0.5mg/kg. The darkest shading denotes the lowest humidity. Stippled areas enclosed by dotted contours denote relatively moist values in the range from 2 to 2.5mg/kg.

Temperatures and specific humidities averaged at 90hPa over January 1997 and January 1998 are compared in Fig. 8. The region where the tropopause is coldest is located much further to the east in 1998, as is the region of warmest sea-surface temperature and strong convection, a characteristic of the El Niño event. As expected, there is a similar shift in the region where the tropopause is driest. Again, the overall moistening due to the 1997 model changes has to be kept in mind. Also included in Fig. 8 are the mean 90hPa temperatures for the Januaries of 1982 and 1983, from the ECMWF re-analyses. There were strong El Niño conditions in the boreal winter of 1983 also, and the

change in tropopause temperature over the tropical Pacific from one year earlier is notably similar to that between the winters of 1997 and 1998. The 90hPa temperatures are, however, markedly colder overall in both 1997 and 1998 than in the two earlier years. They are also colder than in the climatology shown in Fig. 1, as noted earlier for July 1996 and 1997.

Among the marked analysis differences between February 1997 and February 1998 (not shown), temperatures in 1998 were generally colder at 90hPa over the western tropical Indian Ocean, by up to 5°C near Madagascar. Convection tended to dry the base of the stratosphere over this region in 1998, in contrast to the convective moistening in 1997 discussed above. Temperatures were up to 5°C warmer over Micronesia in February 1998 than in February 1997, as will be seen in section 8 for radiosonde measurements at a particular station.

7. DISTRIBUTION OF WATER VAPOUR IN THE STRATOSPHERIC ANALYSES

Winds in the tropical stratosphere are predominantly zonal, with significant vertical shear. In the analyses, a localized area of relatively dry or moist air entering the model stratosphere within the tropics is spread zonally over a time-scale of several weeks as it moves slowly upward. Upward movement and lateral mixing take place on a time-scale of one or more seasons, and are illustrated in Fig. 9 by height/latitude cross-sections of the zonal-mean specific humidity at three-month intervals from 1 April 1996 to 1 January 1998. In this figure, darker shading denotes drier air. The sequence starts soon after humidities larger than 2.5mg/kg were reset to this value at the five uppermost model levels, and variations away from the relatively dry tropical lower stratosphere in the cross-section for 1 April 1996 can be disregarded as transients resulting from the rather arbitrary resetting procedure.

The picture at subsequent times is one of ascent in the tropics, drying in the wintertime Antarctic and latitudinal mixing. Before running through the sequence in more detail, a major deficiency must be noted. The upward transfer in the tropics runs at least twice as fast as indicated either by satellite measurements (Mote *et al.*, 1996) or by estimates of the strength of the global-scale circulation (Holton *et al.*, 1995). Lateral mixing has less time to weaken fluctuations in humidity as they move upward, and the attenuation in the vertical of the annual cycle is accordingly too weak. The excessive rate of vertical transfer is likely to be due principally to an inability of the model's numerical scheme to represent slow mean advection when using coarse vertical resolution, although an erroneously strong mean circulation could be a contributor. In one fifteen-minute model time-step, a typical mean upward motion of around 0.3mm/s would carry a change in humidity upwards through some 30cm, a figure to be compared with a level-spacing of between 2 and 7km in the model between 90 and 10hPa. Given that the model also represents vertical advection by tidal and other wave motions, an unrealistic spreading of humidity in the vertical is perhaps not surprising. A striking improvement in this aspect of model performance will be shown later in a simulation using the 50-level version of the model.

The second cross-section in the sequence shown in Fig. 9, for 1 July 1996, clearly illustrates the upward tropical transfer and the dry Antarctic air formed by condensation as the polar night cools. Over the preceding three months there was significant lateral mixing of dry air into the extratropics at lower stratospheric levels. This mixing appears to have been stronger in the northern (spring/summer) hemisphere, but the mid-latitude lower stratosphere may be moister in the southern hemisphere due to stronger (autumn/winter) descent rather than weaker mixing of dry air in from the tropics. The highest specific humidity is found at upper levels in the Arctic, where mixing is weak due to limited vertical penetration of synoptic- and planetary-scale waves in the summer easterlies, and where meridional transfer by the mean circulation is expected to be weaker than in the winter hemisphere.

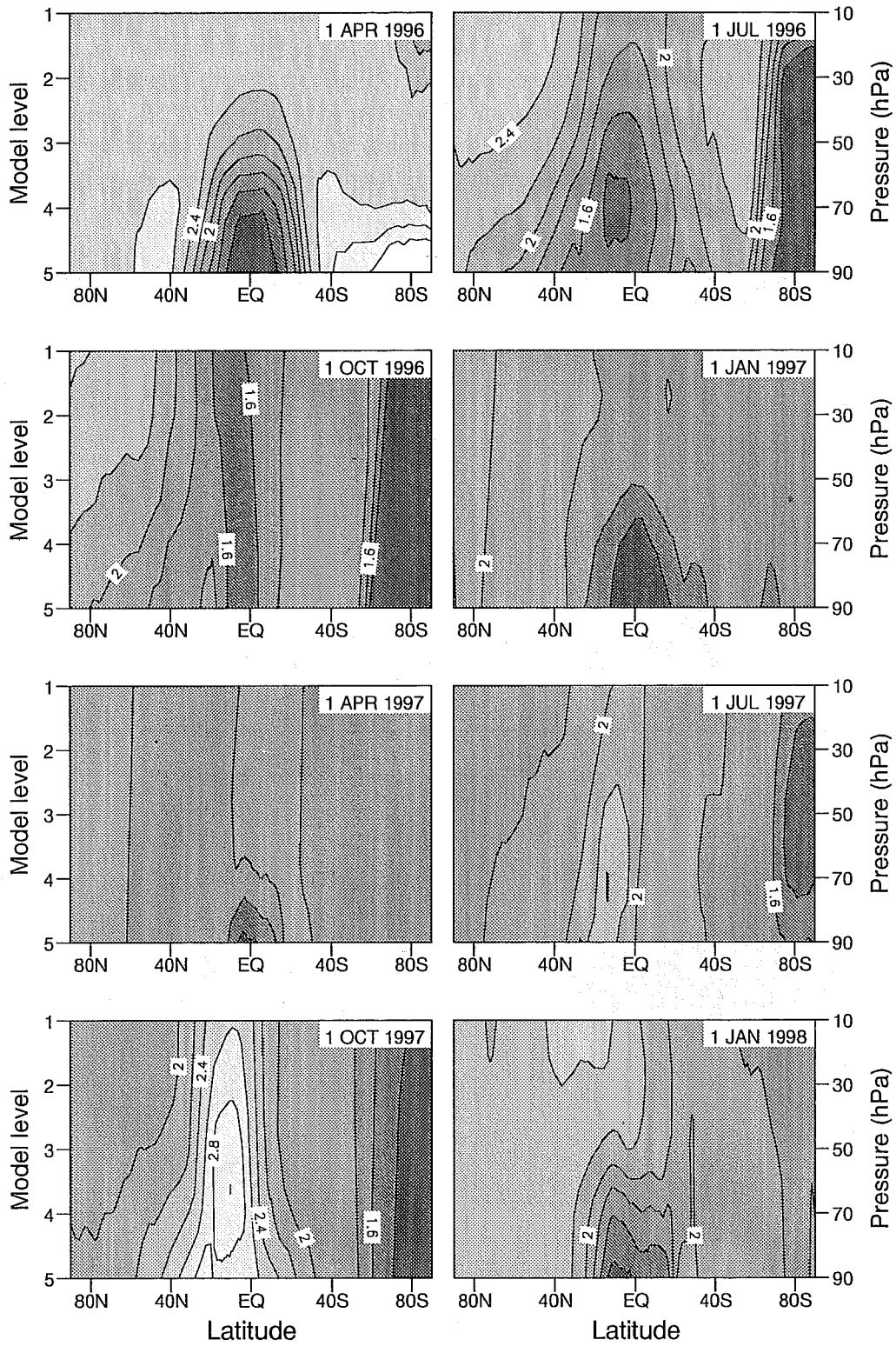

Figure 9 Meridional cross-sections showing zonal means of specific humidity analyses for dates three months apart from 1 April 1996 to 1 January 1998. Darker shading denotes drier values. The contour interval is 0.2mg/kg for values greater than 1.4mg/kg. Values below this limit are denoted by the darkest shading band.

The period from 1 July 1996 to 1 April 1997 is marked by a general homogenization of the stratospheric humidity (in the absence of a parametrization of upper-level moistening by methane oxidation). Some moistening of the southern tropics and subtropics can be seen in April 1997, following the convective moistening at these latitudes near the tropopause in February. The cross-sections in Fig. 9 continue by showing the strong moistening that originates in the northern tropics and subtropics in the summer and early autumn of 1997. The moist air ascends and mixes quite rapidly to give a relatively uniform distribution of humidity in the winter northern hemisphere by the beginning of 1998. Less Antarctic drying is seen in the analyses for the austral winter and early spring of 1997, due both to warmer temperatures (illustrated later) and to the model change in August 1997.

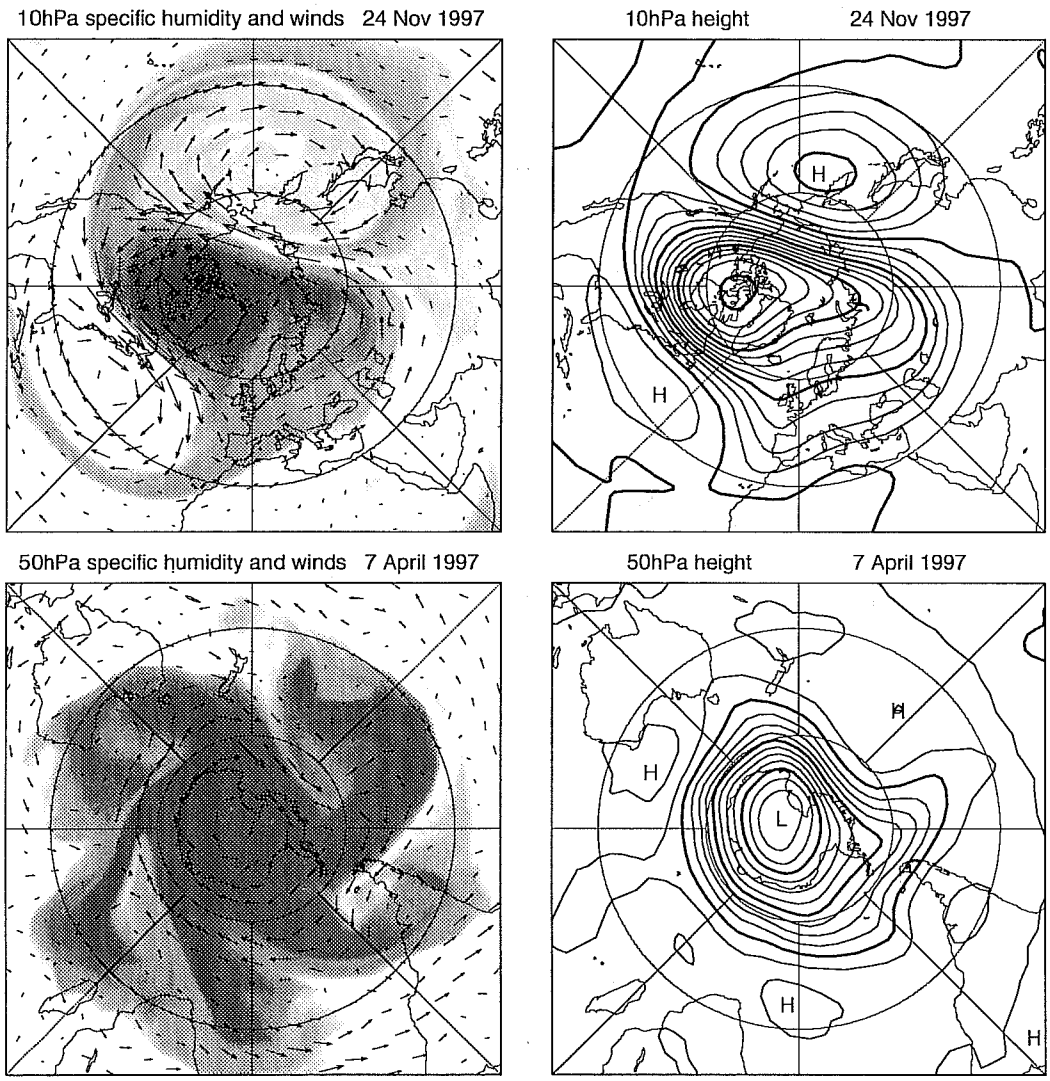

Figure 10 Specific humidity and winds (left) and height (right) of 10hPa northern hemispheric analyses for 12UTC 24 November 1997 (upper) and of 50hPa southern hemispheric analyses for 12UTC 7 April 1997 (lower). The darkest shading denotes the lowest humidities, and shading ranges are from 1.85 to 2.55mg/kg in the upper plot, and from 1.67 to 1.78mg/kg in the lower plot. The contour intervals for height are 160m in the upper plot and 80m in the lower plot, and the scaling of wind arrows differs similarly by a factor of two.

Good indications of the nature of mixing in the extratropical stratosphere has been provided by studies based on the technique of contour-advection, and the injection of substantial aerosol into the stratosphere at 15°N by the eruption of Mt. Pinatubo in June 1991 has provided a fortuitous opportunity for verification (e.g. Plumb et al., 1994;

Rogers et al., 1998). A very similar picture of mixing arises from study of sequences of humidity analyses. Two examples are shown in Fig. 10. Both are from periods with relatively moist air in the subtropics, and shading indicates relatively dry regions.

The upper plot in Fig. 10 shows a striking case of planetary-scale advection and mixing in late November 1997 in the northern hemisphere. The Aleutian High had become well established at 10hPa by this time, and dry air had been extruded completely around it. Intrusion of a stream of relatively moist (unshaded) air into the anticyclone can be seen, and the light shading within the anticyclone is indicative of a mixing of such moist air with filaments of dry air stripped from the vortex. The anticyclone over the Atlantic is weaker in terms of height, but is located further south and has a relatively strong circulation. It is a newly-developed feature that has advected a single streamer of dry air away from the vortex. There is a very close similarity between this situation and one from early December 1991 for which Rogers *et al.*(1998) have presented results on the 700K isentropic surface. The results in Fig. 10 are shown on the isobaric model levels rather than on isentropic levels to avoid contamination by interpolation in a region of limited vertical resolution, 10hPa being the uppermost level of the operational model.

An example of mixing associated with synoptic-scale waves lower in the stratosphere of the southern hemisphere is shown in the lower panels of Fig. 10. The case is from early April 1997, when humidity gradients were relatively low and the equinoctial westerly flow was relatively weak (see figure caption for shading and contouring differences). It is known from the classical work of Charney and Drazin (1961) that there may be significant vertical penetration of the larger synoptic scales for such weak westerly winds. The 50hPa height map shows a marked trough to the west of South America, with weaker troughs upstream and downstream. A more pronounced wave pattern can be seen in the humidity field, which displays evidence of earlier wave activity in the Atlantic and Indian Ocean sectors. It indicates the existence of both intrusion of relatively moist air into the region of strongest circumpolar flow and extrusion of dry air into the subtropics.

Examination of the analyses in the vicinity of the mid-latitude tropopause provides confirmation of the view that stratosphere/troposphere exchange in the extratropics is primarily along isentropes that extend from the troposphere into the stratosphere (Holton *et al.*, 1995). A complete presentation is beyond the scope of this paper, but an illustration of a particular wintertime case is presented here. Fig. 11 shows a cross-section of specific humidity and potential temperature along the dateline from the North Pole to 10°N, for 12UTC 2 January 1998. It has already been shown that humidity in the extratropics was relatively well mixed at 90hPa and above at this time, and the well-mixed stratospheric region can be seen in Fig. 11 to extend down to about the 370K isentropic level. Darker shading in the upper right of the panel denotes drier air in the vicinity of the high tropical tropopause. It is only in a shallow layer in the lowermost stratosphere that the specific humidity increases above typical stratospheric values, associated with the mixing in of air from the more humid troposphere. The lower, darker shading band in Fig. 11 marks the region in which the specific humidity ranges from 3 to 10mg/kg. A marked descending tongue of dry air is evident between 30°N and 40°N, a quite common feature of such sections.

Sequences of analyses interpolated to isentropic surfaces near the tropopause indicate a generally high correlation between specific humidity and potential vorticity in winter and early spring in both hemispheres. Fig. 12 illustrates this with northern hemispheric maps on the 330K surface for 12UTC 2 January 1998. A specific humidity of around 10mg/kg coincides with a potential vorticity of $2 \times 10^{-6} m^2 s^{-1} K\ kg^{-1}$, both indicating where the 330K surface cuts the tropopause. There is considerable similarity between many features in the two fields and evidence of intrusion and extrusion may be seen. Specific humidity provides a sharper picture, partly because it is a variable defined directly on the model grid rather than one (like potential vorticity) derived from the dynamical fields represented spectrally with lower horizontal resolution. More importantly, however, specific humidity is not subject to a non-advective process that significantly changes values in the extratropical lower stratosphere, whereas radiation

changes the potential vorticity of intruded tropospheric air towards typical lower stratospheric values. The humidity field thus provides more of a record of earlier synoptic events than the corresponding potential vorticity field.

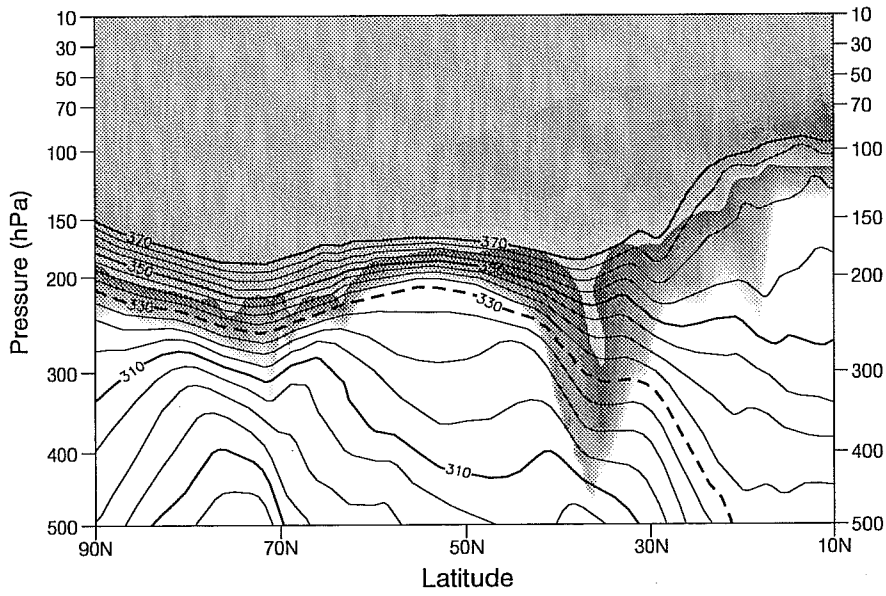

Figure 11 Cross-section showing specific humidity and potential temperature analyses along the dateline for 12UTC 2 January 1998. Shading denotes specific humidity, with changes in intensity every 0.25mg/kg. The two ranges of shading denote values extending (at lower levels) from 10mg/kg (lightest) to 3mg/kg (darkest), and (at upper levels) from 3mg/kg (lightest) to below 1 mg/kg (darkest). Potential temperature is contoured with an interval of 5K for values of 370K and lower. The dashed contour marks the 330K isentrope.

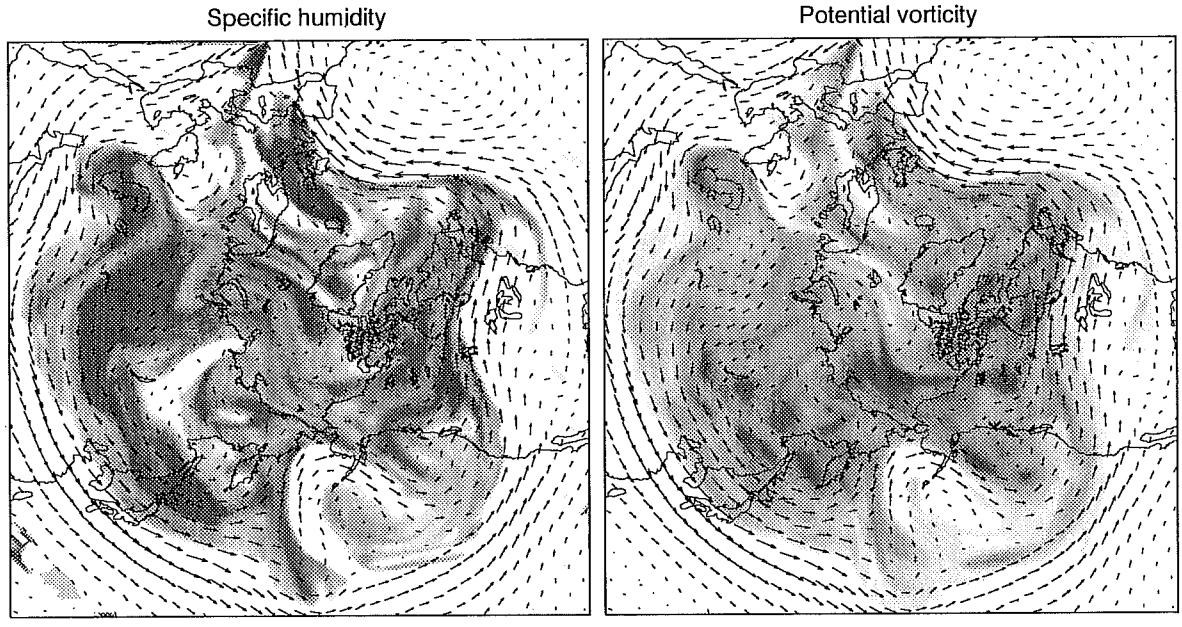

Figure 12 Specific humidity (left), potential vorticity (right) and winds on the 330K isentropic surface for 12UTC 2 January 1998. The shading intensity varies from values of 2 units to 10 units in intervals of 0.25. Lighter shading denotes higher values of humidity and lower values of potential vorticity. Units are mg/kg for specific humidity and $10^{-6}m^2s^{-1}K\ kg^{-1}$ for potential vorticity.

Corresponding northern hemispheric maps for summer and much of autumn do not provide as clear a picture. There is again a marked similarity between local features in the humidity and potential vorticity fields, but the northern upper troposphere is generally moister over southern Asia and the western Pacific, presumably due to the Asian

summer monsoon. There is thus no simple general identification of particular values of potential vorticity and specific humidity near the tropopause. Over Asia, a humidity of up to about 30mg/kg corresponds to a potential vorticity of $2x10^{-6}m^2s^{-1}K\ kg^{-1}$; values of the order of 15-20mg/kg provide a good correspondence for much of the rest of the hemisphere. A value of around 20mg/kg matches this level of potential vorticity in summer near the mid-latitude tropopause in the southern hemisphere. Cross-sections for the northern summer of 1997 show relatively moist air extending to higher levels in the extratropics than in winter, up to 100hPa and above. However, much of the air at the higher levels appears to have entered the stratosphere in the northern tropics and subtropics, as discussed earlier, and then been advected and mixed quite rapidly northward.

The extratropical picture of near-tropopause conditions given here is in broad agreement with that provided by sets of aircraft measurements reviewed by Tuck *et al.*(1997). These showed humidity volume mixing ratios at the mid-latitude tropopause ranging up to 50ppmv in the northern hemisphere, and to about 60% of this value in the southern hemisphere. Water vapour amounts higher than those typical of much of the lower stratosphere were found only at levels below about the 400K isentrope.

8. ACCURACY AND VARIABILITY OF TEMPERATURE ANALYSES

The degree of dryness of the stratosphere both near the tropical tropopause and in the Antarctic polar-night vortex is sensitive to the local temperature, and evidence has been presented of some marked recent deviations in tropopause temperature from the climatology for the period 1979-1993. The accuracy and variability of the temperature analyses are discussed in this section.

We begin with the very cold tropopause temperatures in the region of the "stratospheric fountain" in the boreal winter of 1996/97. Here analysed temperatures fell frequently below -90°C and extreme specific humidities were below 0.5mg/kg. Fig. 13 shows time series of analysed 90hPa temperatures at the positions of two radiosonde stations, Kota Kinabalu at 6°N 116°E in Sabah, Malaysia (northern Borneo) and Truk at 7°N 152°E in the Caroline Islands (northeast of New Guinea). Also shown are the minimum temperatures reported in the radiosonde ascents for these stations received at ECMWF over the Global Telecommunication System (GTS) of the World Meteorological Organisation (WMO). These are generally available twice per day at 00 and 12UTC, and analyses are plotted at these times. The sonde temperatures are plotted only if the ascent received over the GTS included significant-level data extending from below the standard 100hPa level to above the 70hPa level.

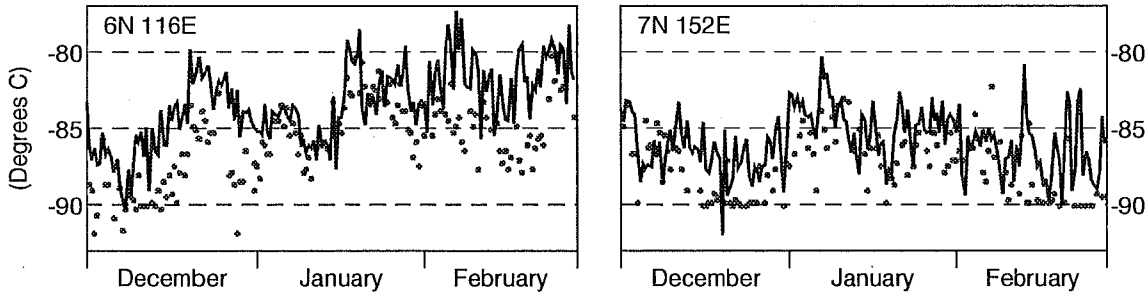

Figure 13 Time series from 1 December 1996 to 28 February 1997 of analysed 00UTC and 12UTC values of 90hPa temperature (continuous lines) at 6°N 116°E (left) and 7°N 152°E (right). Minimum radiosonde temperatures at these locations (stations Kota Kinabalu and Truk, respectively) are denoted by dots.

The 90hPa analysed temperatures are generally higher than the minimum sonde temperatures, by an average of 2.5°C at Kota Kinabalu and 1.8°C at Truk. Comparisons of sonde and analysed temperatures at the standard 100hPa level (discussed later) indicate that only part of this discrepancy can be explained by an overall warm bias of the

analyses in this period. In the observations, the pressure at which the temperature is a minimum varies quite substantially, between 78hPa and 96hPa at Truk in the last two weeks of December, for example. The vertical resolution of the model is only 20hPa around the 90hPa level, and an underestimation of the minimum temperature is thus to be expected. This may result in the analyses providing an underestimation of the drying of air as it enters the stratosphere. However, given the complexity of the actual dehydration process, involving overshooting cumulonimbi, detrainment of cloud ice and so on, it is difficult to estimate how serious a deficiency this is, other than by carrying out experiments with finer vertical resolution near the tropopause. It should also be noted in this context that the ECMWF analysis system is based on use of the reported standard-level geopotential heights from radiosondes rather than the reported temperatures, and that the thermal data from radiosondes used by the analysis are thus restricted to what are in effect mean temperatures for layers such as 70-100hPa and 100-150hPa. A forthcoming move to analyse significant- and standard-level temperatures rather than standard-level heights may bring some improvement near the tropopause, although this will be limited by the broadness of the structure functions used in the analysis (Bouttier et al., 1997; Rabier et al., 1998a).

Regardless of the accuracy of the analyses, the coldness of the reported temperatures and implied dryness are worthy of note. Atticks and Robinson(1983) computed minimum saturation specific humidities from radiosonde ascents between 10°N and 10°S for the period 25 January to 12 February 1979 and found that only 14% of soundings yielded saturation values below 1mg/kg in the longitude range from 150°E to 210°E, with much lower percentages in other longitude bands. Such saturation values correspond to temperatures below -87.1°C at a pressure of 100hPa, and below -88.4°C at a pressure of 80hPa. The minimum temperatures shown in Fig. 13 thus imply saturation specific humidities below 1mg/kg on around 25% of occasions at Kota Kinabalu and 50% of occasions at Truk. A figure of around 40% has been found in similar calculations for Majuro at 7°N 171°E in the Marshall Islands. The maps of monthly-mean specific humidity at 90hPa for December 1996 and February 1997 in Fig. 7 show a considerable area with values under 1mg/kg (indicated by the intermediate level of shading on the maps). The coldest, driest region is centred somewhat south of the observing stations considered here, in a region devoid of radiosonde measurements. In a different period, ship-launched radiosondes from the Central Equatorial Pacific Experiment (CEPEX; Vömel *et al.*, 1995) measured minimum temperatures in the range -87°C to -90°C south of the equator from 7 to 14 March 1993 (Table 1), when the temperatures from the three stations to the north-

Time and date	Location	Minimum T (°C)	Minimum q (mg/kg)	Time and date	Location	Minimum T (°C)	Minimum q (mg/kg)
10UTC 7 March	9°S 160°E	-90	0.4	22UTC 9 March	2°S 169°E	-88	-
7UTC 11 March	2°S 175°E	-89	-	5UTC 12 March	2°S 179°E	-89	0.9
10UTC 12 March	2°S 179°E	-89	-	2UTC 13 March	2°S 178°E	-87	0.8
8UTC 13 March	2°S 177°E	-87	-	23UTC 13 March	2°S 175°E	-87	1.1
8UTC 14 March	2°S 174°E	-88	-	22UTC 14 March	2°S 171°E	-87	0.9

Table 1: Minimum sonde temperatures and minimum specific humidities from CEPEX ascents in March 1993

west considered here were above -87°C in all but one instance. Some of the CEPEX soundings are of particular interest as they provide relatively reliable measurements of humidity from frost-point hygrometers. Minimum

specific humidities have been computed from the reported frost-points and pressures, and Table 1 shows them to be in the range 0.4 to 1.1mg/kg. Discussions of data accuracy and of the implications of these soundings for the mechanisms of stratospheric dehydration are given by Vömel *et al.*(1995)

The cold tropopause temperatures in the winter of 1996/97 exposed radiosonde reporting practice at some stations. Two periods can be seen in Fig. 13 during which minimum temperatures from Truk were reported to be either -89.9°C or -90.1°C on most occasions. The coding of radiosonde temperatures for transmission on the GTS is to an accuracy of 0.2°C, so the suspicion arose that measurements were being limited to a value of -90°C. Enquiries of the radiosonde supplier revealed that there was no known reason why the instrument itself should not provide reliable measurements below -90°C, but that the software applied locally by the operator of the station did indeed limit temperatures to between +50°C and -90°C prior to transmission. It is not known how widespread this practice is, but temperatures apparently limited to -90°C have also been seen in data from Majuro, which is operated by the same weather service as Truk. Temperatures below -90°C can be seen in the series for Kota Kinabalu in Fig. 13.

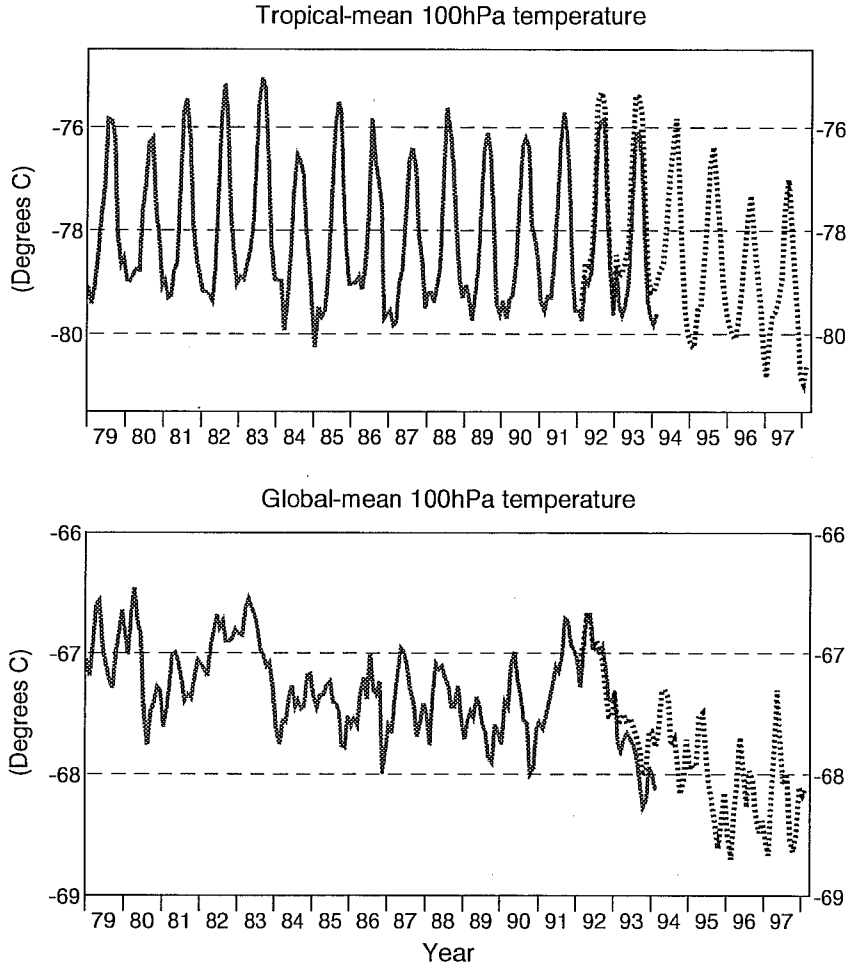

Figure 14 Tropical- mean (upper) and global-mean (lower) 100hPa temperatures averaged at 12UTC for each month from January 1979 to February 1998. The solid line is computed from ECMWF reanalyses for the period up to February 1994. The dotted line is from the operational analyses for the period since January 1992.

The past two years stand out clearly as the coldest in a time series of tropical-mean 100hPa temperature analyses stretching back to 1979, presented in the upper panel of Fig. 14. The series comprises monthly means from the ECMWF re-analyses for the period from January 1979 to February 1994 and from the operational analyses for the

period starting January 1992. The 100hPa temperatures are formed by linear interpolation between values at the model's 90 and 110hPa levels. There is good agreement between the operational analyses and the re-analyses in the overlap period; they differ principally because of a difference in horizontal resolution (T106 for the re-analysis), and because the re-analysis used a later version of the parametrization schemes (operational from April 1995 to January 1996).

A pronounced annual cycle in mean temperature near the tropical tropopause is evident in the upper panel of Fig. 14. Yulaeva *et al.*(1994) argue that this cycle is not primarily a consequence of the annual variation in local tropical convective forcing, but rather is a consequence of the annual variation in the mean tropical ascent that is driven by stratospheric wave activity. This annual variation arises predominantly because of differences in the level of wintertime wave activity between the northern and southern hemispheres. In this respect it is noteworthy that there is no clear signal of interannual variations associated with El Niño events in the series of tropical-mean temperatures shown in Fig. 14.

The conclusions of Yulaeva *et al.*(1994) were based on the observation that the *global-mean* temperature of the lower stratosphere, as inferred from microwave soundings from satellites, showed much less of an annual cycle than the *tropical-mean* temperature. The global-mean ECMWF analyses at 100hPa presented in the lower panel of Fig. 14 confirm this. They do, however, indicate a cooling over the 18-year period. A least squares fit to a linear trend gives a cooling rate of 0.6°C per decade. Such a cooling is of potential significance for the study of climate change (IPCC, 1996), and the trend shown here is consistent with that deduced from radiosonde and microwave soundings alone (Parker *et al.*, 1997) and also with that from the NCEP/NCAR[1] re-analyses (Kalnay *et al.*, 1996; Santer *et al.*, 1998). The corresponding tropical- and global-mean analyses at 70hPa (not shown) exhibit a recent cooling about twice that at 100hPa, with a net linear cooling trend of 0.9°C per decade in the longer-term global mean. They also show a clear signal of short-term warmings due to the volcanic eruptions of El Chicon in early 1982 and Pinatubo in 1991, indications of which may also be seen in the time series for 100hPa shown in Fig. 14.

A question nevertheless remains as to whether the particularly cold tropical tropopause temperatures in the analyses for 1996 and 1997 could to any significant extent be due simply to the change in analysis technique made in January 1996. This is not thought likely, as comparison of OI and 3D-Var analyses made prior to the change showed that the tropical-mean 100hPa temperatures from 3D-Var were only 0.15°C colder than those from OI in a four-week average. Further comparisons have, however, been made with series of radiosonde temperatures.

Pawson and Fiorino(1998) have compared the 100hPa temperature re-analyses for the period 1979-1993 produced by both ECMWF and NCEP. The adequacy of NCEP (and UK Meteorological Office) analyses of tropopause temperature for use in studies of stratospheric water vapour has been questioned by Jackson *et al.*(1998) on the grounds of their warm bias, echoing concerns expressed earlier by Tuck(1994) regarding operational ECMWF analyses from 1987. The tropical-mean 100hPa temperatures from the ECMWF re-analysis are, however, generally colder than the corresponding operational analyses, by an average of 1.1°C in the five-year mean starting 1 July 1985. Moreover, Pawson and Fiorino (*loc. cit.*) found that the ECMWF temperature re-analyses are generally colder than those of NCEP, by up to several degrees locally, and in closer agreement with radiosonde observations. A good mean fit of the recent operational ECMWF analyses to radiosonde temperatures is illustrated below.

Fig. 15 compares 100hPa temperatures at three tropical stations for the period starting January 1994. Two of the stations, Kota Kinabalu and Truk, were chosen again because of their location in the principal region of wintertime

1. National Centers for Environmental Prediction/National Center for Atmospheric Research, USA

drying. The third, Panama at 9°N 80°W, was added to give some geographical diversity. Light dots denote the individual observations and the heavy dotted lines the monthly-mean measured temperatures. As a simple form of quality control, temperatures from radiosonde reports that were either below -95°C or above -60°C were rejected in computing the monthly means. Only twelve observations had to be excluded in this way. The solid lines in Fig. 15 show monthly-means of the operational analyses at the positions of the radiosonde stations.

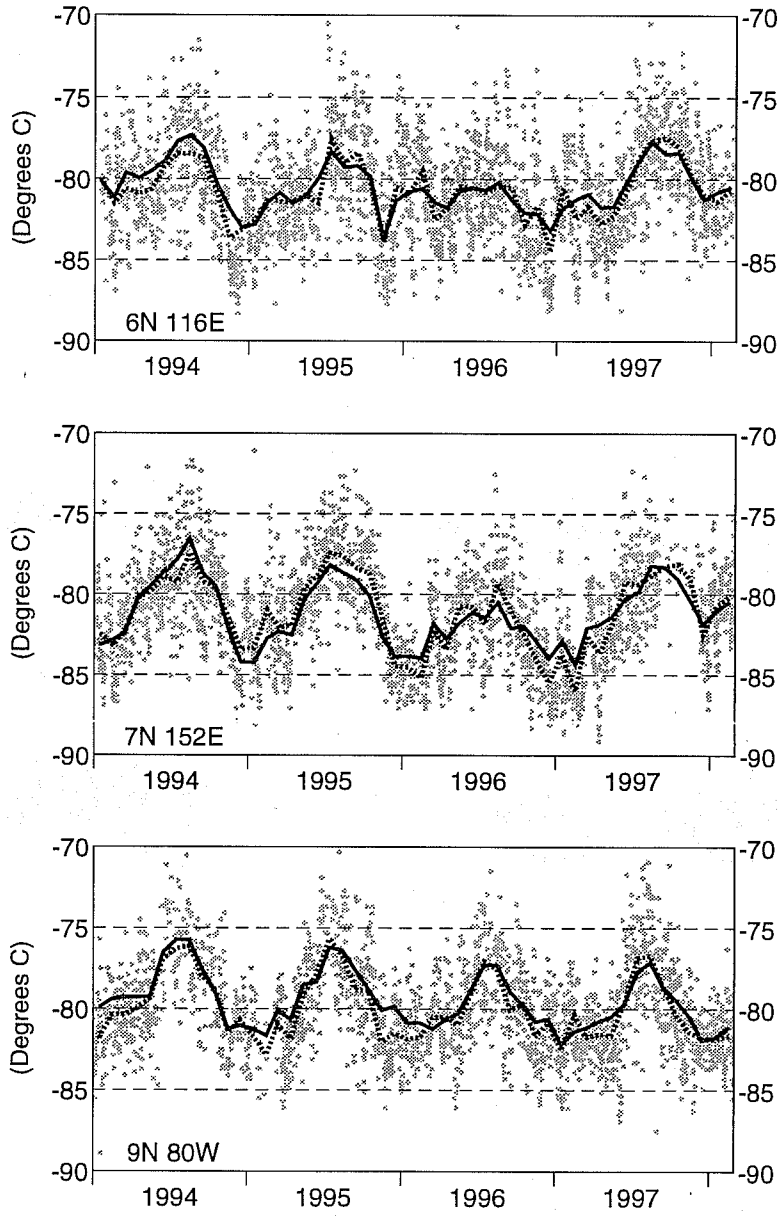

Figure 15 Monthly-mean analysed 100hPa temperatures (solid lines) at 6°N 116°E (upper), 7°N 152°E (middle) and 9°N 80°W (lower), and monthly-mean radiosonde temperatures at these locations (dotted lines; stations Kota Kinabalu, Truk and Panama, respectively) from 1 January 1994 to 28 February 1998. The grey dots denote the individual (00 and 12UTC) radiosonde measurements.

There is clearly a good general agreement between the analysed and observed monthly-mean 100hPa temperatures shown in Fig. 15. In the mean over the full 50-month period, differences are only 0.21°C at Kota Kinabalu, -0.06°C at Truk and 0.44°C at Panama. The analysis bias is slightly worse in the first 25 (pre 3D-Var) months, with mean

differences of 0.3°C, -0.3°C and 0.6°C at the three stations. Note, however, that on average the (3D-Var) analysis underestimated by about 1°C the particularly cold temperatures observed at Truk in the winter of 1996/97. The radiosonde measurements (and analyses) clearly indicate relatively cold summer temperatures at Kota Kinabalu and Truk in 1996. In 1997 and early 1998 the shift in temperature pattern associated with the latest El Niño takes these two stations to normal summer values and then to relatively warm winter values. At Truk, the mean measured temperature is some 5°C warmer in February 1998 than in February 1997. A decline in summertime maximum temperatures at Panama is evident over the four years.

Longer time-series of average winter and summer 100hPa temperatures from the radiosondes at Kota Kinabalu, Truk and Panama are shown in Fig. 16. The period starts with the summer of 1980. These series provide a better indication of how unusually cold some recent seasons have been. They also give an impression of a general cooling trend over the period, as discussed above for tropical and global means. The warmth of the mean temperature at Truk in the El-Niño winter of 1982/83 compared to the two preceding winters (and the comparison with the latest three winters) is worthy of note. Care must, however, be taken in interpreting series such as these from individual stations, not only because of effects of El Niños and volcanic eruptions, but also because of possible effects of instrument changes.

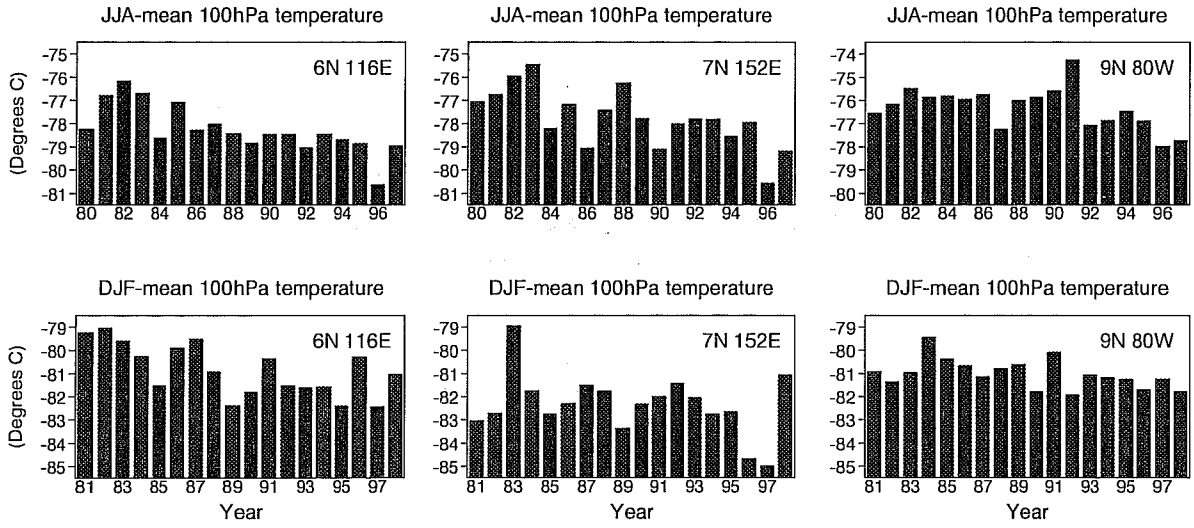

Figure 16 Seasonal-mean 100hPa radiosonde temperatures at Kota Kinabalu (6°N 116°E; left), Truk (7°N 152°E; middle) and Panama (9°N 80°W; right) for June-August (upper) from 1980 to 1997 and for December-February (lower) from 1980/81 (labelled 81) to 1997/8.

The comparison of analysed temperatures with radiosonde measurements at individual stations has been complemented by computing statistics of the fit of the analyses to all the tropical radiosonde measurements used in the data assimilation. As noted above, the ECMWF analysis system is based on use of the reported standard-level geopotential heights. The archived "feedback" information produced for each observation used during the data assimilation thus enables a comprehensive comparison to be made between analysed and observed geopotential thicknesses, which can be converted easily to layer-averaged virtual temperatures. In the case of 4D-Var, each observation is compared with the final-trajectory forecast valid for the time the observation was made. Almost all radiosonde reports are timed either at one of the main synoptic hours (mostly 00 and 12UTC) or one hour earlier (e.g. Järvinen and Undén, 1997). The fit to radiosonde data is thus evaluated at or near the middle of the six-hour forecast that determines the evolution of the humidity analysis in the stratosphere. To summarize the current position, statistics have been computed for 00 and 12UTC 4D-Var analyses produced between September 1997 and February 1998. Over this period the analyses have a cold bias of 0.5°C for the 100-70hPa layer and a

warm bias of 0.3°C for the 150-100hPa layer. Corresponding standard deviations are 1.3°C for 100-70hPa and 1.1°C for 150-100hPa. Comprehensive sets of such statistics for the ECMWF (OI) re-analyses have been compiled by Uppala (1997). The biases are quite variable over the fifteen-year period, despite use of a fixed data assimilation system. They are, however, generally below 0.4°C in magnitude near the tropical tropopause. For OI (and 3D-Var) these statistics apply at the start time of the background forecast; biases at the six-hour forecast range are typically at least some 50% larger. This should be taken into account when comparing with figures from 4D-Var.

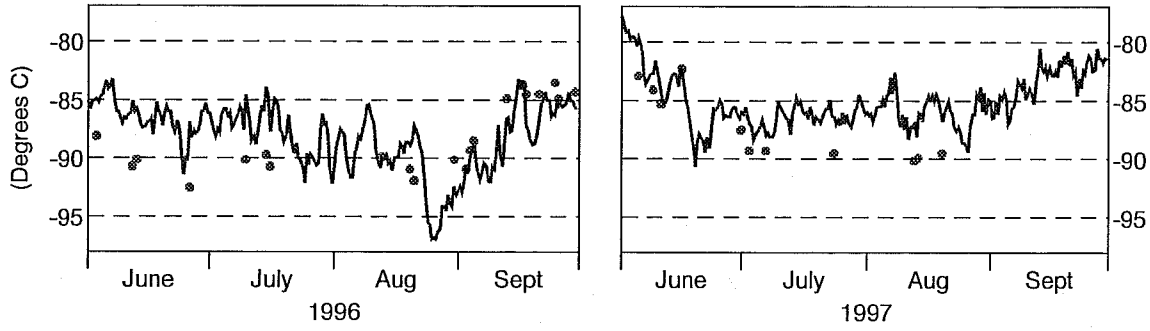

Figure 17 Time series from 1 June to 30 September of analysed 50hPa temperatures at the South Pole (continuous lines) and corresponding radiosonde measurements (dots), for 1996 (left) and 1997 (right).

We conclude this section with a brief comparison of analysed temperatures and radiosonde observations in the wintertime stratosphere at the South Pole. Conditions at and above the Amundsen-Scott base in winter are far less conducive to frequent stratospheric reports, but temperature measurements at 50hPa are received on the GTS from this station about six times per month on average. Fig. 17 compares these measurements with 50hPa analyses for the winters of 1996 and 1997. 1997 is generally warmer than 1996 in both analyses and radiosonde observations, consistent with the analyses being moister in 1997, as noted earlier. In both years, however, the analyses tend to be warmer than the observations. This is seen also in the ten-year means for the period 1988-1997 shown in Table 2. These indicate a warm bias of about 2°C in mid-winter. Here the analysed values have been taken from the re-analyses for 1988-1993 and from operations for 1994-1997. The mean radiosonde temperature of -90.3°C at 50hPa in August corresponds to a saturation specific humidity of 1.1 mg/kg.

Month	Number of sonde measurements (1988-1997)	Mean radiosonde temperature (1988-1997)	Mean analysed temperature (1988-1997)	Mean simulated temperature
June	65	-86.0°C	-84.2°C	-84.9°C
July	65	-89.9°C	-87.9°C	-89.5°C
August	61	-90.3°C	-88.2°C	-92.2°C
September	44	-85.0°C	-83.7°C	-90.7°C

Table 2: Mean radiosonde, analysed and simulated 50hPa temperatures at South Pole

9. STRATOSPHERIC HUMIDITY IN MULTI-YEAR SIMULATIONS

Two-year simulations have been produced using the 31- and 50-level versions of the model. The operational ECMWF OI analysis for 12UTC 1 January 1995 was chosen as initial conditions, and the stratospheric humidity was thus set to 2.5mg/kg except where the saturation value was lower. Initial winds and temperatures above 40hPa

for the 50-level version were taken from the UARS analyses produced routinely by the UK Meteorological Office (Swinbank and O'Neill, 1994). Sea-surface temperatures were set periodically to the evolving NCEP analyses for the period 1995-1996 (Reynolds and Smith, 1994). The 50-level simulation was subsequently extended for a further six years as it was found to be producing a realistic-looking QBO. Sea-surface temperatures for the extra six years were prescribed by repeating six times the values for 1996. The version of the parametrizations used was that operational immediately prior to the model change in August 1997. These simulations thus suffer from a stratospheric drying of 10-15% due to the inaccuracy in the calculation of saturation vapour pressure discussed earlier.

Fig. 18 shows height-time cross-sections of the tropical-mean specific humidity from both two-year simulations. The height range covers that portion of the tropical stratosphere resolved by the 31-level version; output from this version has been interpolated linearly to the levels of the 50-level version prior to contouring. At the lowest level shown, close to the tropical tropopause, both versions of the model produce a realistic simulation of the annual cycle in specific humidity, with a range of about 1.8-2.8mg/kg in the first year and 1.9-2.6mg/kg in the second year. As in the 31-level operational analyses, the upward propagation of the annual variation is too rapid in the 31-level simulation, the first minimum at the 10hPa level following just six months or so after the first minimum at the tropopause.

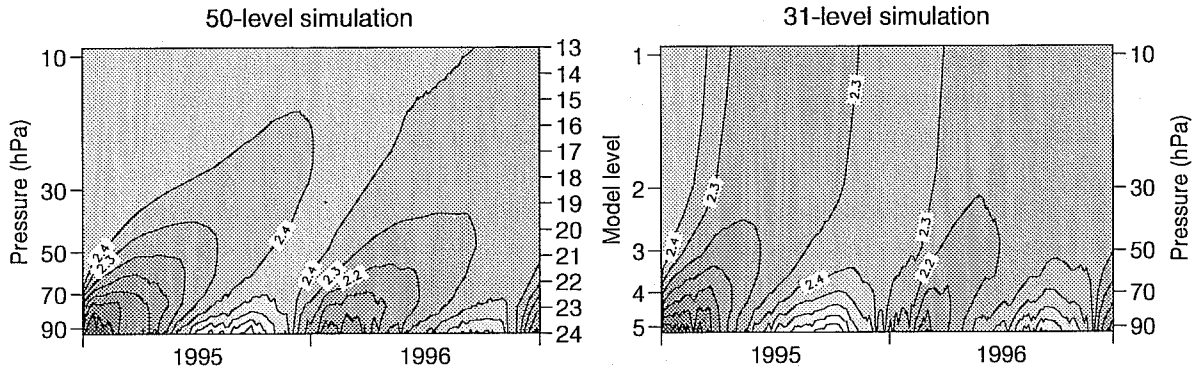

Figure 18 Height/time cross-sections showing the evolution of the tropical-mean specific humidity between about 90 and 10hPa over two-year simulations using 50-level (left) and 31-level (right) model versions. Darker shading denotes drier values. The contour interval is 0.1mg/kg.

In contrast, the 50-level simulation provides a quite realistic representation of the "tape recorder" effect. The upward transfer of layers of relatively dry and moist air occurs much more slowly than in the 31-level simulation, and the mean rate of around 11km per year (about 0.35mm/s) is only some 20-30% faster than indicated by the measurements from UARS discussed by Mote et al.(1996). There is much more attenuation of the annual signal as it moves upwards more slowly in the 50-level simulation. This attenuation is stronger for the moistening introduced in the boreal summer than for the drying introduced in the boreal winter. There is also a more rapid ascent in boreal winter than in summer, as indicated for example by the shape of the 2.4mg/kg contour for the 50-level simulation in Fig. 18.

Fig. 19 shows a similar height-time cross-section of tropical-mean specific humidity, but this time for the whole eight years of the 50-level simulation, and for the full model domain above the tropical tropopause. There is little interannual variability in the drying that occurs at the tropopause each boreal winter, the specific humidity typically falling to around 1.8mg/kg early each year. It must, however, be kept in mind that this simulation used the same annual cycle in sea-surface temperature for each year other than the first. Some variability is nevertheless apparent in the moistening in boreal summer and early autumn, with the specific humidity failing to reach 2.4mg/kg in the

seventh year of integration, although it rises to a more typical maximum value above 2.5mg/kg in the eighth year. There is an overall upward spreading of dry air at a rate which slows in later years.

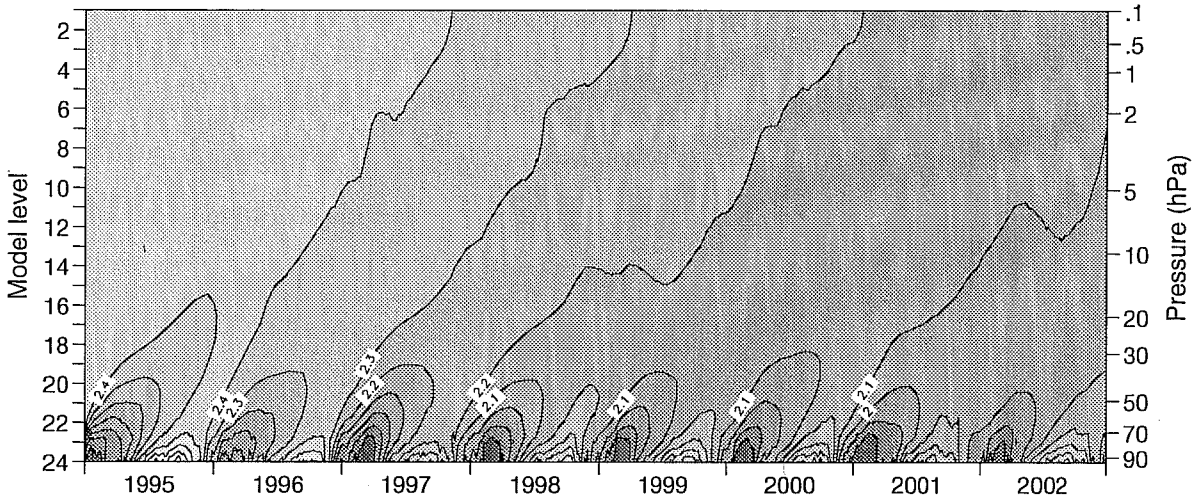

Figure 19 Height/time cross-section showing the evolution of the tropical-mean specific humidity between about 90 and 0.1hPa over eight years of simulation using the 50-level model version. Darker shading denotes drier values. The contour interval is 0.1mg/kg.

Meridional cross-sections of zonal-mean specific humidity are presented in Fig. 20. The panels show sections early in January and July for the first, third, fifth and seventh year of integration. The slow ascent of dry air in the tropics is accompanied by lateral mixing, qualitatively as seen earlier for the 31-level operational analyses. There is also a quite substantial drying in winter (and early spring) over Antarctica, strongest between about 30 and 50hPa. The dry air subsequently descends and mixes into middle latitudes, leaving the lower stratosphere generally drier in the southern than the northern hemisphere. The mean extratropical descent also brings down relatively moist air from the uppermost levels, especially in high latitudes of the winter hemisphere. This air has not been moistened as in reality by methane oxidation (Lahoz *et al.*, 1996), but is moist because it has been least changed since the start of the simulation.

The broadly realistic multi-year simulation of mean humidity near the tropical tropopause is indicative of a reasonable simulation of tropopause temperatures. Eight-year January- and July-mean simulated temperatures at the model level closest to 90hPa are shown in Fig. 21. There is particularly close agreement between the January map and the corresponding climatological mean map shown in Fig. 1, with differences smaller than 2°C over most of the tropics. The simulation for July is generally colder than the climatology, but warmer than the mean analyses for this month in 1996 and 1997. It is in fact difficult to know quite what temperatures the model should be producing, given the uncertainties arising from recent trends in tropopause temperature.

Simulated eight-year monthly-mean 50hPa temperatures at the South Pole for June to September are included in Table 2. These temperatures match mean radiosonde temperatures quite accurately in June and July, but are too cold in August, and even more so in September. The model warms rapidly by a realistic amount in October, but evidently underestimates the late winter and early spring warming over Antarctica. The continuing cold temperatures are conducive to an additional, erroneous drying of the southern lower stratosphere.

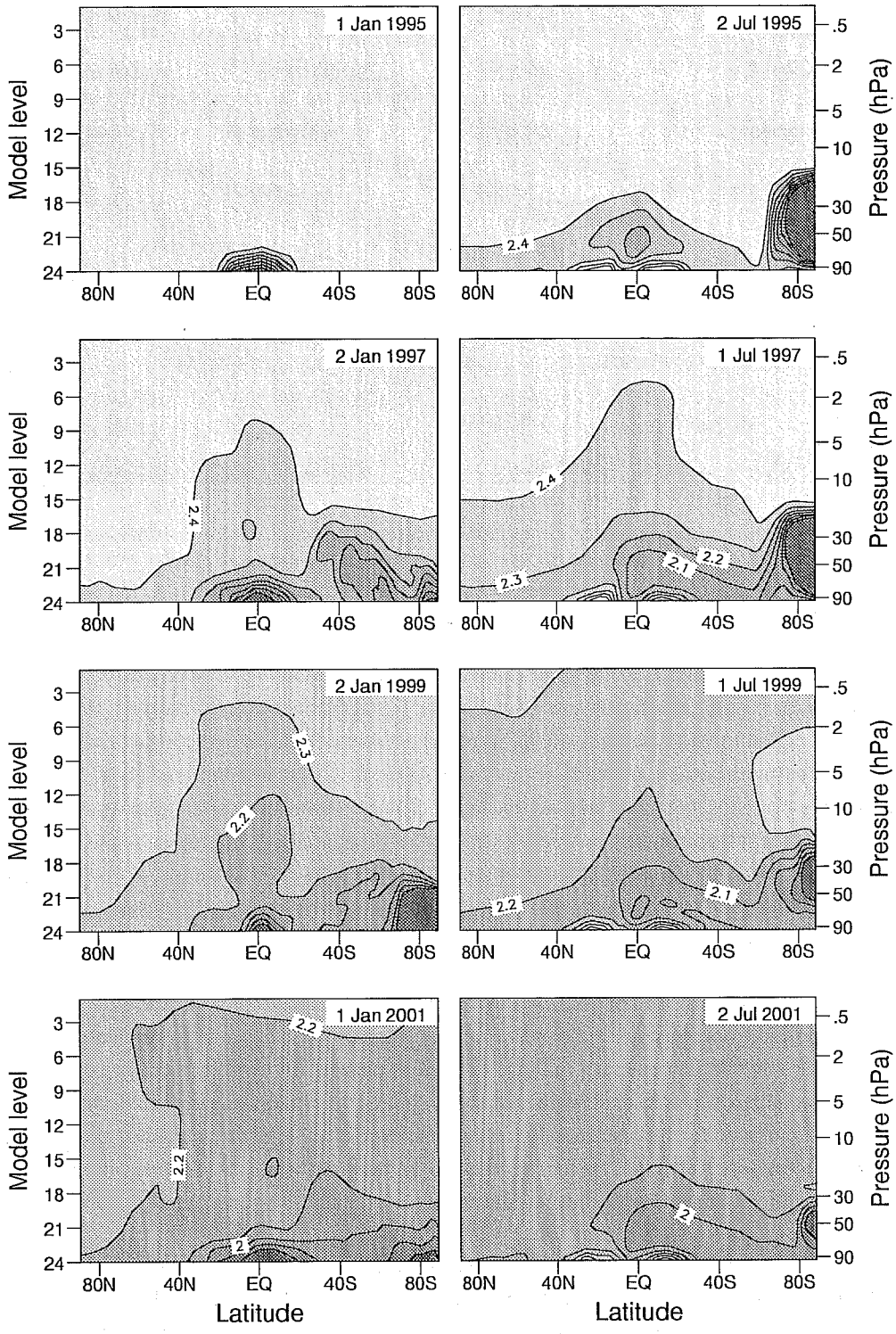

Figure 20 Meridional cross-sections of zonal-mean specific humidity at the beginning of January (left) and July (right) for the first and every subsequent second year of the 50-level simulation. Darker shading denotes drier values. The contour interval is 0.1mg/kg for values greater than 1.8mg/kg. Values below this limit are denoted by the darkest shading band.

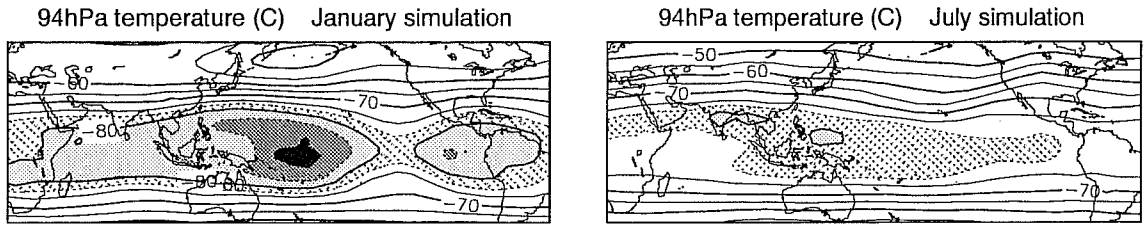

Figure 21 Temperature at the model level close to 94hPa averaged for January (left) and July (right) from the 50-level simulation. Contouring and shading are as in Fig. 1.

10. CONCLUDING DISCUSSION

The results presented in this paper demonstrate a current capability to model stratospheric water vapour that has clearly advanced substantially from the position reviewed by Holton *et al.*(1995). They also demonstrate that a modern data assimilation system can provide analyses of temperature near the tropical tropopause that have substantially lower biases than has generally been the case in the past. They should thus help allay ongoing concerns as to the adequacy of operational analyses of near-tropopause temperature for use in studies of lower stratospheric water vapour, such as expressed recently by Jackson *et al.* (1998). The temperature analyses may also usefully complement long series of station or satellite measurements in providing a global picture of trends in tropopause and lower stratospheric temperatures. The ECMWF analyses presented here indicate in particular that the tropical tropopause has been substantially colder over the past two years than in any other year in the period since 1979.

Recent operational ECMWF humidity analyses appear to be in reasonable agreement with retrievals from UARS measurements near the tropopause, with regard both to overall amount of water vapour and to its geographical and seasonal distribution. Improvements in detail are likely to result from many of the planned developments discussed below, but the analyses appear already to have a useful role to play alongside satellite and *in situ* measurements for the study of tropopause and lower stratospheric humidity. They also provide a qualitative description of behaviour at higher levels which is in accord with general understanding of the distribution of water vapour in the stratosphere. Considerable quantitative improvement can be expected from using finer and more extensive vertical resolution in the model and from including a representation of moistening by methane oxidation.

Analyses near the tropical tropopause are, as expected, driest where the tropopause is coldest. This occurs in the boreal winter, in a region which usually lies over the convectively-active deep tropical western Pacific, the region termed the "stratospheric fountain" by Newell and Gould-Stewart (1981). The region of strongest convective activity and coldest tropopause temperature moves to the central and eastern Pacific when sea-surface temperatures warm there at times of El Niño. The specific humidity is lowered in the analyses by repeated instances of highly local dehydration associated with the occurrence of deep convection in the background or final-trajectory forecasts of the 3D- or 4D-variational data assimilation. Dry air spreads relatively rapidly in the zonal direction as it is generally carried slowly upwards by mean ascent in the tropical stratosphere. Local regions of ascent and descent forced by convective heating in the troposphere may, however, play some role in the immediate vicinity of the tropopause. This vertical motion diminishes substantially with increasing height near the tropopause, and inadequate vertical resolution in the model may result in analyses with too great a vertical penetration of the tropospherically-forced circulations. Nevertheless, the analyses for the boreal summer and autumn of 1996 show dry air that originates from deep convection over Indonesia being advected eastward and downward over the Indian Ocean, giving a distribution of humidity consistent with the climatology constructed by Jackson *et al.*(1998) from

HALOE retrievals. The local convectively-driven circulations may thus play a part in determining quite how much of the relatively dry (or moist) air at the base of the tropical stratosphere is actually taken up by the slow wave-driven stratospheric circulation.

Moistening of the base of the tropical (and subtropical) stratosphere must also be taken into account in forming a comprehensive picture of stratospheric water vapour. The analyses show this to be predominant in the boreal summer and early autumn, in accord with observations. The summertime specific humidity is a maximum over the southern Asian land mass. Sequences of daily maps do not indicate a clear direct link between the moistening in this region and pronounced convective rainfall, and diagnosis is needed to determine to what extent the net moistening here is due to advection by the regional-scale convectively- and orographically-forced ascent associated with the Asian summer monsoon. Summertime moistening occurs also in the analyses over central America, where the tropopause is relatively warm and there is ascent in the climatological mean. Significant moistening of the outer tropics and subtropics apparently more directly linked to the presence of strong convection is evident in late summer and early autumn in both hemispheres, especially in the regions of tropical cyclonic activity.

The relatively moist air that enters the lowermost stratosphere in the outer tropics and subtropics in summer and early autumn is well placed both for early mixing into the nearby extratropics by synoptic-scale disturbances and for subsequent mixing by planetary-scale disturbances in late autumn and winter. In contrast, the dry air that is introduced in the deep tropics predominantly in boreal winter is less exposed to mixing with the extratropics. The annual cycle in the outer-tropical and subtropical moistening is thus likely to be attenuated much more strongly in the vertical than the annual cycle in the deep-tropical drying. This is indeed seen in the 50-level simulations presented in this paper. It is seen also in latitude/time sections of HALOE water-vapour retrievals at different levels in the stratosphere (Evans and Harries, 1996; Evans, personal communication). In addition, the entry of moist air into the stratosphere at outer-tropical and subtropical latitudes and its subsequent mixing into the neighbouring extratropics is consistent with aircraft measurements of chemical composition which indicate that air in the stratosphere of each hemisphere comes predominantly from the troposphere of the same hemisphere (Tuck *et al.*, 1997).

A more quantitative analysis of a number of the more reliable aspects of the analyses and the multi-year simulations is desirable. This is beyond the scope of this paper, and would in any case be best applied to several forthcoming datasets, rather than those studied here. Specifically, results from two major programmes will become available for study in addition to the future operational analyses. The first of these will comprise a series of seventeen-year 50-level simulations using sea-surface temperatures for the period 1979-1995. These simulations are being carried out as part of the second phase of the Atmospheric Model Intercomparison Project (Gates, 1992), and the range of diagnostics to be produced during the simulations will be much more comprehensive than produced during the pilot 50-level simulation reported here. The second programme will comprise a new analysis of the period from 1957 to the present day, extending and enhancing the original 15-year ECMWF re-analysis. This too will use the 50-level resolution. These programmes should provide a good basis for the study of interannual variability and trends.

A number of the planned changes to the operational ECMWF forecasting system should improve the representation of stratospheric water vapour in the analyses. The 50-level resolution is currently being used in data-assimilation and medium-range forecast trials, and is expected to become operational within a few months. It would clearly be desirable to accompany this with introduction of some representation of moistening by methane oxidation, if only by including a simple relaxation towards higher specific humidity at the uppermost levels of the model. There may be improvement near the tropopause from a planned change to use standard- and significant-level temperatures and winds in the analysis, rather than the present standard-level geopotentials and winds. In the longer term, increased vertical resolution near the tropical tropopause will be investigated, and further benefit should be derived from

ongoing refinements in parametrization, especially related to deep convection, stratiform cloud processes and radiation.

Attention will be paid to ensuring consistent physical balance in the data assimilation. Convective activity in the background (or final-trajectory) forecasts of the data assimilation plays a very important role in both hydration and dehydration of the analyses near the tropical tropopause. This convective activity may be either uncharacteristically weak (a "spin-up" problem) or strong (a "spin-down" problem) in these very short-range forecasts. This happens when the analysis modifies the background thermodynamic profile or low-level moisture convergence in a way which systematically disrupts the physical balance preferred by the model, even if the modification is justified by observations. Stendel and Arpe (1997) and Kållberg (1998) document the problem for the ECMWF re-analysis: convective precipitation in general exhibits a spin-up, and is 15% larger over the oceans in the forecast range from twelve to twenty-four hours than in the six-hour background forecasts. Conversely, current operational ECMWF forecasts typically show a spin-down of tropical rainfall averaging about 10%.

A relevant new development is the extension of the forecasting system to include ozone as an analysed model variable. Information on ozone will be extracted variationally from HIRS[1] radiances, and later from radiances measured by new operational instruments such as SEVIRI[2] and IASI[3]. Use may also be made of ozone products retrieved from various other types of satellite measurement. The lower stratosphere is distinguished from the upper troposphere by its lower humidity, its higher ozone and its higher potential vorticity. Development of a multivariate analysis which links ozone, water vapour and the dynamical variables offers promise not only for better definition of water vapour and ozone near the tropopause, but also for the improvement of weather forecasts that can be expected from a better dynamical definition of the near-tropopause region.

There is scope also for a more direct improvement of the humidity analysis in the upper troposphere and lower stratosphere from assimilation of additional humidity-sensitive measurements. Work is well in progress on the use of observations from the water-vapour channel of Meteosat and of similar data from other geostationary satellites. Use of the model humidity field above 300hPa in the fitting of the TOVS and future ATOVS[4] radiances is also under investigation. In the longer term interferometers such as IASI will provide data with improved vertical resolution near the tropopause. In addition, there are opportunities for validation of the analyses by detailed comparison with measurements from experimental instruments on commercial aircraft and research satellites, which may open paths to eventual assimilation of such data.

ACKNOWLEDGEMENTS

Stimulating comments and promptings from Tony Hollingsworth, Michael McIntyre, Martin Miller and Adrian Tuck are gratefully acknowledged. Many colleagues at ECMWF are thanked for their advice and technical assistance.

1. High resolution InfraRed Sounder, a component of the TOVS and ATOVS instrument groups
2. Spinning Enhanced Visible and InfraRed Imager
3. Infrared Atmospheric Sounding Interferometer
4. Advanced TOVS

APPENDIX A CALCULATION OF THE SATURATION VAPOUR PRESSURE

The saturation vapour pressure, $e_s(T)$, is defined in the parametrization schemes of the ECMWF model by the Tetens formula:

$$e_s(T) = a_1 e^{a_3\left(\frac{T-T_0}{T-a_4}\right)}$$

Until August 1997, the parameters used operationally were a_1=611.14Pa, a_3=17.269 and a_4=35.86K for the value over water, and a_3=21.875 and a_4=7.66K for the value over ice. T_0=273.16K and T is in degrees Kelvin. The variational data analysis scheme used a different representation, based directly on integration of the Clausius-Clapeyron equation, assuming latent heats to be linearly dependent on temperature (Courtier *et al.*, 1991).

Table 3 shows various representations of the saturation vapour pressure (in units of Pa) as a function of T (°C, first column). Unbracketted values are over water for temperatures above 0°C, and over ice otherwise. Values over water for temperatures between 0°C and -30°C are given in brackets. The second and third columns show respectively the Tetens formula as used until August 1997 in the ECMWF parametrizations and the result of integrating the Clausius-Clapeyron equation as used in the analysis scheme. These values should be compared with the (WMO-

T(°C)	Tetens	Clausius-Clapeyron	Smithsonian	ASHRAE	AERKi	BUCK
50	12341.	12281.	12340.	12350.		12369
40	7378.7	7355.4	7377.7	7383.8		7384.2
30	4244.9	4235.9	4243.0	4246.2		4243.5
20	2339.4	2335.7	2337.3	2338.9		2337.3
10	1228.6	1227.3	1227.2	1228.0		1227.6
0	611.1 (611.1)	611.1 (611.1)	610.7 (610.8)	(611.2)	611.2	(611.2)
-10	259.6 (285.9)	260.0 (286.6)	259.7 (286.3)	(286.2)	259.7	(286.5)
-20	102.8 (124.7)	103.3 (125.6)	103.2 (125.4)	(125.4)	103.1	(125.4)
-30	37.66 (50.21)	37.99 (51.00)	37.98 (50.88)	(50.86)	37.97	(50.73)
-40	12.62	12.81	12.83		12.83	
-50	3.819	3.918	3.935		3.938	
-60	1.029	1.070	1.080		1.082	
-70	.2424	.2570	.2615		.2618	
-80	.0489	.0532	.0547		.0547	
-90	.0082	.0092	.0097		.0096	
-100	.0011	.0013	.0014		.0014	

Table 3: Alternative evaluations of saturation vapour pressure ($e_s(T)$, in Pa) as a function of temperature, T.

recommended) values given in the Smithsonian Meteorological Tables (1951), shown in the fourth column, and the more modern ASHRAE values over water (Gueymard, 1993; fifth column). The Tetens formula underestimates $e_s(T)$ by 10-15% for temperatures in the range -80 to -90°C. The Clausius-Clapeyron integration gives better values

for low temperatures, but it still underestimates by 5% at -90°C and gives slightly poorer results for warm temperatures.

Two other columns are shown in Table 3. AERKi is the result of a formula of Tetens form, but with coefficients different to those used in the model prior to August 1997. This version of the formula was recommended by Alduchov and Eskridge (1996) for the saturation vapour pressure over ice. These authors' best values for the formula over water do not compare well with our current model values for warm temperatures, presumably because they come from a best fit of the value over water for a temperature range down to -40°C. Several alternative sets of coefficients have been examined, the most promising being the set recommended by Buck(1981). Buck's formula has the property of continuity with AERKi at T=0°C, as both formulae have the same value for a_1.

The Buck and AERKi parameters are a_1=611.21Pa, a_3=17.502 and a_4=32.19K for the saturation vapour pressure over water, and a_3=22.587 and a_4=-0.7K for the value over ice. The operational ECMWF model was changed to use these new parameters on 27 August 1997.

In the model the saturation vapour pressure that is actually used is the value over water for temperatures above 0°C and the value over ice for temperatures lower than -23°C. For intermediate "mixed-phase" temperatures, T (in degrees Kelvin), the value is given by

$$e_s(T) = e_{si}(T) + (e_{sw}(T) - e_{si}(T))\left(\frac{T - T_i}{T_0 - T_i}\right)^2$$

where $e_{si}(T)$ is the value over ice, $e_{sw}(T)$ is the value over water, and T_0 - T_i = 23K. Until 27 August 1997, the operational variational analysis code simply took the saturation vapour pressure to be the value over water for temperatures above 0°C and the value over ice for temperatures lower than 0°C. On 27 August, the analysis scheme was changed to use the same formulation as the model, including both use of the new version of the Tetens formula and use of the model's mixed-phase formulation.

REFERENCES

Alduchov, O.A., and Eskridge, R.E. (1996) Improved Magnus form approximation of saturation vapour pressure. *J. Appl. Meteorol.*, 35, 601-609.

Andersson, E., and Järvinen, H. (1998) Variational quality control. Submitted to *Q. J. R. Meteorol. Soc.*.

Atticks, M.G., and Robinson, G.D. (1983) Some features of the structure of the tropical tropopause. *Q. J. R. Meteorol. Soc.*,**109**, 295-308.

Beljaars, A.C.M. (1995) The impact of some aspects of the boundary-layer scheme in the ECMWF model. *Proceedings of 1994 ECMWF Seminar on Parametrization of Sub-grid Scale Physical Processes*, 125-161.

Bermejo, R., and Staniforth, A. (1992) The conversion of semi-Lagrangian advection schemes to quasi-monotone schemes. *Mon. Wea. Rev.*, **120**, 2622-2632.

Bouttier, F., Derber, J., and Fisher, M. (1997) The 1997 revision of the J_b term in 3D/4D-Var. *ECMWF Tech. Memo.*, **238**, 54pp.

Brewer, A.W. (1949) Evidence for a world circulation provided by measurements of the helium and water vapour

distribution in the stratosphere. *Q. J. R. Meteorol. Soc.*, **75**, 351-363.

Buck, A. (1981) New equation for computing vapor pressure and enhancement factor. *J. Appl. Meteorol.*, **20**, 1527-1532.

Charney, J.G., and Drazin, P.G. (1961) Propagation of planetary-scale disturbances from the lower to the upper atmosphere. *J. Geophys. Res.*, **66**, 83-109.

Courtier, P., and Naughton, M. (1994) A pole problem in the reduced Gaussian grid. *Q. J. R. Meteorol. Soc.*, **120**, 1389-1407.

Courtier, P., Freydier, C., Geleyn, J.-F., Rabier, F., and Rochas, M. (1991) The ARPEGE project at Météo-France. *Proceedings of 1991 ECMWF Seminar on Numerical Methods in Atmospheric Models*, Vol. II, 192-231.

Courtier, P., Andersson, E., Heckley, W., Pailleux, J., Vasiljevic, D., Hamrud, M., Hollingsworth, A., Rabier, F., and Fisher, M. (1998) The ECMWF implementation of three dimensional variational assimilation (3D-Var). Part I: Formulation. *Q. J. R. Meteorol. Soc.*, **124**, in press.

Dobson, G.M.B.,Brewer, A.W., and Cwilong, B.M. (1946) Meteorology of the lower stratosphere. *Proc. R. Soc. London*, **A185**,144-175.

Evans, S.J., and Harries, J.E. (1996) Variability of water vapour near the tropopause from HALOE. *Proceedings of XVIII Quadrennial Ozone Symposium*, xx-yy.

Fisher, M., and Courtier, P. (1995) Estimating the covariance matrices of analysis and forecast error in variational data assimilation. *ECMWF Tech. Memo.*, **220**, 26pp.

Gates, W.L. (1992) AMIP: The Atmospheric Model Intercomparison Project. *Bull. Amer. Meteorol. Soc.*, **73**, 1962-1970.

Gibson, J.K., Kållberg, P., Uppala, S., Hernandez, A., Nomura, A., and Serrano, E. (1997) ERA description. *ECMWF Re-Analysis Project Report Series*, **1**, 72pp.

Gueymard, C. (1993) Assessment of the accuracy and computing speed of simplified saturation vapor equations using a new reference dataset. *J. Appl. Meteorol.*, **32**, 1294-1300.

Harries, J.E. (1997) Atmospheric radiation and atmospheric humidity. *Q. J. R. Meteorol. Soc.*, **123**, 2173-2186.

Holton, J.R., Haynes, P.H., McIntyre, M.E., Douglas, A.R., Rood, R.B., and Pfister, L. (1995) Stratosphere-troposphere exchange. *Rev. Geophys.*,**33**, 403-43

Hortal, M.(1994) Recent studies of semi-Lagrangian advection at ECMWF. *ECMWF Tech. Memo. No. 224*, 37pp.

Hortal, M., and Simmons, A.J.(1991) Use of reduced Gaussian grids in spectral models. *Mon. Wea. Rev.*, **119**, 1057-1074.

IPCC (1996) Climate change 1995: The science of climate change. J.T. Houghton, L.G. Meira Filho, B.A. Callander, N. Harris, A. Kattenberg and K. Maskell (Eds.), Cambridge Univ. Press, 572pp.

Jackson, D.R., Driscoll, S.J., Highwood, E.J.,Harries, J.E., and Russell, J.M. III (1998) Troposphere to stratosphere transport at low latitudes as studied using HALOE observations of water vapour, 1992-1997. *Q. J. R. Meteorol. Soc.*, **124**, 169-192.

Järvinen, H., and Undén, P. (1997) Observation screening and background quality control in the ECMWF 3D-Var data assimilation system. *ECMWF Tech. Memo.*, **236**, 33pp

Kållberg, P. (1998) Aspects of the re-analysed climate. *ECMWF Re-Analysis Project Report Series*, **2**, 89pp.

Kalnay, E., Kanamitsu, M., Kistler, R., Collins, W., Deaven, D., Gandin, L., Iredell, M., Saha, S., White, G., Woolen, J., Zhu, Y., Chelliah, M., Ebisuzaki, W., Higgins, W., Janowiak, J., Mo, K.C., Ropelewski, C., Wang, J., Leetma, A., Reynolds, R., Jenne, R., and Joseph, D. (1996) The NCEP/NCAR 40-year reanalysis project. *Bull. Amer. Meteorol. Soc.*, **77**, 437-471.

Lahoz, W.A., O'Neill, A., Heaps, A., Pope, V.D., Swinbank, R., Harwood, R.S., Froidevaux, L., Read, W.G., Waters, J.W., and Peckham, G.E. (1996) Vortex dynamics and the evolution of water vapour in the stratosphere of the southern hemisphere. *Q. J. R. Meteorol. Soc.*, **124**, 423-450.

Lorenc, A.C. (1981) A global three-dimensional multivariate statistical interpretation scheme. *Mon. Wea. Rev.*, **109**, 701-721.

Lott, F., and Miller, M.J. (1997) A new subgrid-scale orographic drag parametrization: Its formulation and testing. *Q. J. R. Meteorol. Soc.*, **123**, 101-127.

McNally, A.P., and Vesperini, M. (1996) Variational analysis of humidity information from TOVS radiances.*Q. J. R. Meteorol. Soc.*, **122**, 1521-1544.

Morcrette, J.J. (1990) Impact of changes in the radiation transfer parametrization plus cloud optical properties in the ECMWF model. *Mon. Wea. Rev.*, **118**, 847-873.

Mote, P.W., Rosenlof, K.H., McIntyre, M.E., Carr, E.S., Gille, J.C., Holton, J.R., Kinnersley, J.S., Pumphrey, H.C., Russell, J.M. III, and Waters, J.W. (1996) An atmospheric tape recorder: The imprint of tropical tropopause temperatures on stratospheric water vapour. *J. Geophys. Res.*, **101D**,3989-4006.

Newell, R.E., and Gould-Stewart, S. (1981) A stratospheric fountain? *J. Atmos. Sci.*, **38**, 2789-2796.

Ovarlez, J., and van Velthoven, P. (1997) Comparison of water vapour measurements with data retrieved from ECMWF analyses during the POLINAT experiment. *J. Appl. Meteorol.*, **36**, 1329-1335.

Parker, D.E., Gordon, M., Cullum, D.P.N., Sexton, D.M.H., Folland, C.K., and Rayner, N. (1997) A new global gridded radiosonde temperature data base and recent temperature trends.*Geophys. Res. Lett.*, **24**, 1499-1502.

Pawson, S., and Fiorino, M. (1998) A comparison of reanalyses in the tropical stratosphere. Part 1: Thermal structure and the annual cycle. Submitted to *Clim. Dyn.*.

Plumb, R.A., Waugh, D.W., Atkinson, R.J., Newman, P.A., Lait, L.R., Schoeberl, M.R., Browell, E.V., Simmons, A.J., and Loewenstein, M. 1994 Intrusions into the lower stratospheric arctic vortex during the winter of 1991/92. *J. Geophys. Res.*, **99**, 1089-1105.

Rabier, F., McNally, A., Andersson, E., Courtier, P., Undén, P., Eyre, J., Hollingsworth, A., and Bouttier, F. (1998a) The ECMWF implementation of three-dimensional variational assimilation (3D-Var). Part II: Structure functions. *Q. J. R. Meteorol. Soc.*, **124**, in press.

Rabier, F., Järvinen, H., Klinker, E., Mahfouf, J.-F., Simmons, A., Andersson, E., Bouttier, F., Courtier, P., Fisher, M., Hamrud, M., Haseler, J., Hollingsworth, A., Isaksen, L., Saarinen, S., Temperton, C., Thépaut, J.-N., Undén, P., and D. Vasiljevic (1998b) The ECMWF operational implementation of four dimensional variational assimilation. Part I: Experimental results with simplified physics. Submitted to *Q. J. R. Meteorol. Soc.*.

Reynolds, R.W., and Smith, T.M. (1994) Improved global sea surface temperature analysis using optimal interpolation. *J. Clim.*, **7**, 929-948.

Ritchie, H., Temperton, C., Simmons, A., Hortal, M., Davies, T., Dent, D., and Hamrud, M. (1995) Implementation of the semi-Lagrangian method in a high resolution version of the ECMWF forecast model. *Mon. Wea. Rev.*, **123**, 489-514.

Rodwell, M.J., and Hoskins, B.J. (1996) Monsoons and the dynamics of deserts. *Q. J. R. Meteorol. Soc.*, **122**, 1385-1404.

Rogers, H.L., Norton, W.A., Lambert, A., and Grainger, R.G. (1998) Transport of Mt. Pinatubo aerosol by tropospheric synoptic-scale and stratospheric planetary-scale waves. *Q. J. R. Meteorol. Soc.*, **124**, 193-209.

Santer, B.D., Hnilo, J.J., Boyle, J.S., Doutriaux, C., Fiorino, M., Parker, D.E., Taylor, K.E., and Wigley, T.M.L. (1998) Uncertainties in "observational" estimates of temperature change in the free atmosphere. Submitted to *J. Geophys. Res.*.

Simmons, A.J. (1982) The forcing of stationary wave motion by tropical diabatic heating. *Q. J. R. Meteorol. Soc.*, **108**, 503-534.

Simmons, A.J., and Burridge, D.M. 1981 An energy and angular-momentum conserving vertical finite-difference scheme and hybrid vertical coordinates. *Mon. Wea. Rev.*, **109**, 758-766.

Simmons, A.J., and Strüfing, R. 1983 Numerical forecasts of stratospheric warming events using a model with a hybrid vertical coordinate. *Q. J. R. Meteorol. Soc.*, **109**, 81-111.

Simmons, A.J., and Temperton, C. (1996) Stability of a two-time-level integration scheme for gravity-wave motion. *Mon. Wea. Rev.*, **125**, 600-615.

Stendel, M., and Arpe, K. (1997) Evaluation of the hydrological cycle in reanalyses and observations. *Max-Planck Institute for Meteorology Report,* **228**, 52pp.

Swinbank, R., and O'Neill, A. (1994) A stratosphere-troposphere data assimilation system. *Mon. Wea. Rev.*, **122**, 686-702.

Tiedtke, M. (1989) A comprehensive mass flux scheme for cumulus parametrization in large-scale models. *Mon. Wea. Rev.*, **117**, 1779-1800.

Tiedtke, M. (1993) Representation of clouds in large-scale models. *Mon. Wea. Rev.*, **121**, 3040-3061.

Tuck, A.F. (1994) Use of ECMWF products in stratospheric measurement campaigns. *Proceedings of 1993 ECMWF Workshop on the Stratosphere and Numerical Weather Prediction*, 73-105.

Tuck, A.F., Baumgardner, D., Chan, K.R., Dye, J.E., Elkins, J.W., Hovde, S.J., Kelly, K.K., Loewenstein, M., Margitan, J.J., May, R.D., Podolske, J.R.,Proffitt, M.H., Rosenlof, K.H., Smith, W.L., Webster, C.R., and Wilson, J.C.(1997) The Brewer-Dobson circulation in the light of high-altitude *in situ* aircraft observations. *Q. J. R. Meteorol. Soc.*, **123**, 1-69.

Untch, A. (1998) Simulation of the quasi-biennial oscillation with the ECMWF model. *Research activities in atmospheric and oceanic modelling, WMO, Geneva*, **27**, 6.26-6.27.

Uppala, S. (1997) Observing system performance in ERA. *ECMWF Re-Analysis Project Report Series*, **3**, 261pp.

Viterbo, P., and Beljaars, A.P.M. (1995) An improved land surface scheme in the ECMWF model and its validation. *J. Clim.*, **8**, 2716-2748.

Vömel, H., Oltmans, S.J., Kley, D., and Crutzen, P.J. (1995) New evidence for the stratospheric dehydration mechanism in the equatorial Pacific. *Geophys. Res. Lett.*, **22**, 3235-3238.

Williamson, D.L. (1990) Semi-Lagrangian moisture transport in the NMC spectral model. *Tellus*, **42A**, 413-428.

Yulaeva, E., Holton, J.R., and Wallace, J.M. (1994) On the cause of the annual cycle in the tropical lower stratospheric temperature. *J. Atmos. Sci.*, **51**, 169-174.